

# VIBRATION-TO-ELECTRICITY CONVERSION: A REVIEW OF ELECTROMAGNETIC, ELECTROSTATIC AND PIEZOELECTRIC ENERGY HARVESTERS

Hamid Khan<sup>\*1</sup>, Farid Ullah Khan<sup>2</sup>

<sup>\*1,2</sup>Department of Mechatronics Engineering, University of Engineering and Technology, Peshawar, 25000, Pakistan

DOI: <https://doi.org/10.5281/zenodo.16778478>

## Keywords

Energy harvester, vibration, non-resonant, electromagnetic, electrostatic, piezoelectric, WSN

## Article History

Received on 18 May 2025

Accepted on 18 June 2025

Published on 27 June 2025

Copyright @Author

Corresponding Author: \*

Hamid Khan

## Abstract

Recent years have seen a surge in research into vibration energy harvesters (VEHs) due to the potential for them to power low-energy devices and wireless sensor nodes (WSNs). These include vibration electromagnetic energy harvester (VEMEHs), vibration electrostatic energy harvesters (VESEHs) and vibration piezoelectric energy harvesters (VPEEHs). Recent developments in VEHs are discussed in depth in this article. In terms of operating frequency range, frequency bandwidth, size, output voltage, power density, power output value, and vibration levels, all of the VEHs have been investigated and documented. In addition, the reported VEHs are classified as either resonance based VEHs or non-resonant VEHs as per their functioning mechanism. The VEMEHs that have been documented range in size from very small (0.032 cm<sup>3</sup>) to very big (about 1600 cm<sup>3</sup>) harvesters. When evaluated based on output voltage, the VEMEHs reported in this review could generate output voltage ranging from as low as 0.13 mV to as high as 5700 mV. Likewise, VEMEHs that have been described can provide output powers ranging from 0.00096 μW to 74,000 μW. The power densities of the VEMEHs that have been recorded range from 5 × 10<sup>-7</sup> μW/cm<sup>3</sup> to 1073 μW/cm<sup>3</sup>. The VEMEHs that have been described have power per acceleration ranging from 0.016 × 10<sup>-3</sup> μW/g to 129.8 mW/g. In addition, the power density per acceleration ranges from 5 × 10<sup>-7</sup> μW/g.cm<sup>3</sup> to 1.87 mW/g.cm<sup>3</sup> for the VEMEHs that have been reported. The described vibration energy harvesters span a vast array of sizes and power outputs. As an illustration, research has demonstrated that a petite 1 cm<sup>3</sup> device may provide 0.75 μW average harvested power, whereas a bigger 68.96 cm<sup>3</sup> harvester can reach a maximum power of 74000 μW. The VESEHs that are documented range in size from very small (0.0025 cm<sup>3</sup>) to big (about 2.25 cm<sup>3</sup>) harvesters. Likewise, VESEHs that have been described can provide output powers ranging from pW to 600 μW. The power densities of the VESEHs that have been recorded range from 0.52 μW/cm<sup>3</sup> to 19616 μW/cm<sup>3</sup>. The VESEHs that have been described have power per acceleration vary from 0.082 μW/g to 81.76 μW/g.

The VPEEHs that have been documented range in size from very small (0.00042 cm<sup>3</sup>) to comparatively quite big (about 540 cm<sup>3</sup>) harvesters. Likewise, VPEEHs that have been described can provide output powers ranging from as low as 0.9 μW to as high as 321 mW. The power densities of the VPEEHs that have been recorded range from 1.61 μW/cm<sup>3</sup> to 82307 μW/cm<sup>3</sup>. The VESEHs that have been described have power per acceleration ranging from a very low value of

0.75 $\mu$ W/g to a very high value of 214000 $\mu$ W/g.

In order to assess their effectiveness, vibration energy harvesters (VEHs) were compared across six critical parameters: operating frequencies range, harvester size, power output, operational acceleration, power-to-acceleration ratio, and power density.

## INTRODUCTION

The widespread availability of mobile devices and wireless sensors has led to significant technological advancements across various fields. Wireless sensing electronics are now utilized in diverse applications, including environmental monitoring (such as temperature, humidity, and light levels), structural health monitoring of infrastructures like bridges and high-rise buildings, asset tracking and surveillance, industrial and medical equipment diagnostics, and sensing in military and aerospace systems[1]. Wireless Sensor Nodes (WSNs) monitor physical and environmental characteristics in these applications. A typical WSN has a sensor unit, signal processing and conditioning module, microprocessor,

onboard memory, transceiver, and power management module [2]. Some commercially offered sensors with their type, make and model, measurement range, working voltage, current and power level requirements have been listed in Table I. The temperature sensors consume 13.8 to 247  $\mu$ W of power. Documented pressure sensors need 3–240 mW of power. Similar to acceleration sensors, they use 0.45 to 72.8 mW. The current needs for temperature, pressure, and acceleration sensors are 6  $\mu$ A to 45  $\mu$ A, 1 mA to 10 mA, and 0.2 mA to 13.25 mA, respectively. Temperature, pressure, and acceleration sensors require 1.8 V to 5.5 V, 3 V to 24 V, and 2.25 V to 5.5 V.

Table 0 :Commercially available sensors

Sensors	Manufactured By	Model	Measurement Range	Required Voltage (V)	Current ( $\mu$ A)	Power ( $\mu$ W)	Ref.
Temperature Sensors	Texas Instruments	LMT85	-50 to 150	1.8 to 5.5	8.1	14.5 to 44.5	[3]
	Microchip	MCP9701A	-40 to +125	3.1 to 5.5	6	18.6 to 33	[4]
	Microchip	MCP9700	-40 to +150	2.3 to 5.5	6	13.8 to 33	[5]
	Analog Devices	TMP35	+10 to +125	2.7 to 5.5	50	135 to 275	[6]
	Sensirion	STS30	-40 to +125	2.7 to 5.5	6.6	17.8 to 36.3	[7]
	Texas Instruments	TMP101	-55 to +125	2.7 to 5.5	45	121.5	[8]
Pressure Sensors	Changzhou Leili	QYK	0.1 to 3.2	4.75 to 5.25	10	47.5 to 52.5	[9]
	TE Connectivity	MS4525DO	1 to 150 psi	3.3 to 5.0	-	-	[10]
	Micro Sensor Co., Ltd.	MPM286	0 to 3.5	-	2	-	[11]
	Shanghai TM Sensor	Ns-P22	0 to 60	24	10	240	[12]
	Dallas Semiconductors	DS18B20	-55 to +125	3 to 5.5	1	3 to 5.5	[12]
Acceleration Sensors	Analog Devices	ADXL425	$\pm 1.7 / \pm 5 / \pm 18$	5	0.7	3.5	[13]
	Analog Devices	ADXL357	$\pm 10 / \pm 20 / \pm 40$	2.25 to 5	0.2	0.45 to 1	[14]
	Analog Devices	ADXL251	$\pm 60 / \pm 120 /$	3.135	6	18.8	[15]

	Texas Instruments	DRV-ACC16	±16	3.5 to 5.5	10	35 to 55	[16]
	Microchip	MM7150	± 2	5.5	13.25	72.8	[17]
	STMicroelectronics	LIS3L02AL	± 2	3.3	-	-	[18]

In most cases, batteries power Wireless Sensor Nodes. However, depending on usage and energy consumption, these batteries must be recharged or replaced periodically, which can be time-consuming and impractical, especially in remote areas. These systems employ rechargeable or non-rechargeable batteries. Non-rechargeable batteries must be changed after usage. Rechargeable batteries may usually be recharged 500 times. A growing variety of wireless applications are suitable for energy harvesting devices that store energy in rechargeable batteries [18]. Nickel Cadmium (NiCd) batteries are reliable but have a low energy density. For applications requiring high discharge rate, long life, and low cost, NiCd batteries are used. Power tools, video cameras, and biomedical equipment are main uses. Toxic elements in NiCd batteries affect the environment. Domestic appliances,

industrial machines, cars, and bridges cause vibrations and their frequency range.

Refrigerator casings accelerate at 0.002 g ( $g = 9.8 \text{ m/s}^2$ ), while kitchen blender casings accelerate at 0.653 g. These appliances range in frequency from 1 Hz (found in split AC outdoor units) to 520 Hz (found in the back of window AC units). Car acceleration ranges from 1.04 g (highway freight vehicles) to 2.514 g (city Ford vans). These cars also vibrate from 0 to 500 Hz. These bridges have vibration accelerations from 0.0025 g (Seoha grand bridge for light trains, South Korea) to 0.061 g (Golden Gate Bridge for vehicles, San Francisco) and frequencies from 0 to 80 Hz.

The associated frequency from each source of vibration has also been mentioned in the table II.

**Table 0I:** Different vibrational sources, together with the accelerations and frequencies of those sources

Source of Vibration	Frequency Range (Hz)	Governing Frequency (Hz)	Maximum Acceleration (g)	Ref.
Small microwave oven	-	120	0.229	[27]
Bread maker	-	120	0.105	[27]
Clothe dryer	-	59	0.433	[27]
Casing of kitchen blender	40-250	216	0.653	[27]
Vacuum cleaner	-	100	0.157	[27]
Notebook computer while reading CD	-	75	0.06	[28]
Casing of refrigerator	-	100	0.002	[28]
Windows Air-conditioner backside	10-520	120	0.234	[29]
Outdoor of split AC (old)	1-130	120	0.3	[29]
Outdoor of split AC (new)	1-130	17	0.06	[29]
Washing machine	10-100	11	0.238	[29]
Car engine compartment	-	200	1.22	[30]
Human walking	-	2-3	0.306	[31]
Wooden deck when people walking	-	385	0.132	[31]

Door frame as the door closes	-	125	0.306	[32]
Cargo trucks on highways	10-500	10 to 20	1.04	[33]
Ford van (on city roads)	0-200	10 to 20	2.514	[33]
Honda light car	0-200	1 to 10	1.399	[34]
Golden gate bridge for vehicles ( San	0-5	0 -1.5	0-0.061	[35]
Seoha grand bridge for light trains	1 to 10	2 to 4	0.0025-0.018	[35]
Huanghe cable bridge for vehicles	1 to2	-	0.015	[35]
Xiangjiang grand bridge	1 to 80	40	0.0093-0.026	[35]

The harvester's peak output is at its resonant frequency for linear resonators. Minor excitation frequency changes can worsen it [36]. Since most viable vibration sources are frequency-varying or random, increasing the vibration energy harvester's bandwidth has been one of the biggest challenges before its widespread use [36], [37].

Recently, this field has made great development, as shown in this overview. This page summarises electro-magnetic, electro-static, and piezo-electric vibration-based energy harvesting systems. The discussion includes frequency tuning [38], [39], multimode and nonlinear electromagnetic energy harvesting [40], [41], frequency up-conversion [42], [43], [44], [45], and spring-less wide-band electromagnetic energy harvesting [46], [47], [48], [49], [50]. The review assessed each technique's benefits and uses in various situations.

### I. OBJECTIVES

This research aims to uncover the latest research methods and viable solutions. If one knows the newest viable option, implementing a new solution may be possible. Based on operating frequencies range, harvester size, power output, operational acceleration, power-to-acceleration ratio, and power density, all three harvesting systems are analysed for pros and cons. This study compares harvesting methods and explains which is best. The results section summarises the comparison and suggests the optimum harvesting method for powered WSN and IoT applications.

### II. VIBRATION ELECTROMAGNETIC ENERGY HARVESTERS (VEMEHs)

Electromagnetic devices operate on the basis of electromagnetic induction and govern by Faraday's law of induction. Relative movement between a coil and a magnet results in generating an electromotive force. For

better efficiency, electromagnetic devices need high frequency and high acceleration. It offers advantages such as various device architectures, multiple fabrication processes, low output impedance, and a wide range of operating frequencies and accelerations, rendering it more appropriate for residential, industrial, and health monitoring applications. Furthermore, VEMEHs generate relatively low output voltages and elevated current levels.

### III. (A) RESONANT VEMEHs

By way of electromagnetic induction and mechanical resonance, a resonant VEMEH transforms mechanical vibrational energy into electrical energy. The vibration amplitude of the magnet and coil rises when the frequency of the external source corresponds with the natural resonance frequency of the mechanical system, therefore optimising the rate of change in the magnetic field and hence the induced voltage. This resonance phenomena boosts the mechanical vibration to electrical energy conversion.

John Heit et al. [51] described a frequency-tunable Vibration Energy Micro-Electro-Mechanical Harvester (VEMEH) in Fig.1. This harvester's simple and small mechanical mechanism changed structural stiffness to modify its resonance frequency over a wide range. The device consisted of two sets of N52 Neodymium magnets (6.35 mm<sup>3</sup>), a square coil, and a spring structure to modulate resonance frequency. The peak power output at 0.2 g was 340  $\mu$ W for harmonic up-sweeps. The VEMEH's operating frequency was tunable between 32 and 85 Hz, according to [51] tests. The voltage against frequency plot assessed the device's bandwidth at 5 Hz.

Fig. 2 shows Takahiro Sato et al.'s non-linear wide-band VEMEH for random vibrations [52]. Environmental vibrations change the magnets' locations relative to the coil, affecting magnetic flux and causing EMF. Because

the magnetic material inside a coil directed flux lines, it could increase magnetic flux. The strong attraction between the magnets and the magnetic material caused nonlinear oscillations in the cantilever beam, allowing it to respond to more frequencies. Thus, power production exceeding 0.1 mW was maintained from 20–160 Hz.

Podder et al. [53] designed a nonlinear VEMEH for low-frequency applications, shown in Fig. 3. This device uses a 300 μm thick folded cantilever construction to improve energy harvesting in low-frequency situations. The folded cantilever structure's centre piece was fixed at the bottom, while external vibrations allowed the rest to swing. The harvester used opposite magnetic fields to create a high

magnetic flux gradient area. Four NdFeB magnets (4 mm x 2 mm x 1 mm) were epoxy-bonded to the FR4 slot's edges. The slot between the magnets held a 2500-turn coiled copper coil with 1.15 mm internal and 4 mm external diameter. A Neodymium (NdFeB) magnet (4 mm x 1 mm x 1 mm) was installed at the cantilever tip, facing a sixth (4 mm x 2 mm x 1 mm) magnet directly in front of it. The system's dynamic response was nonlinear because these magnets repelled one other. Changing the spacing between the two repulsing magnets enhanced bandwidth and non-linearity. With a wide bandwidth of 8 Hz, the device generated 19.3 μW peak power under 1.5 g acceleration and 1 kΩ load.

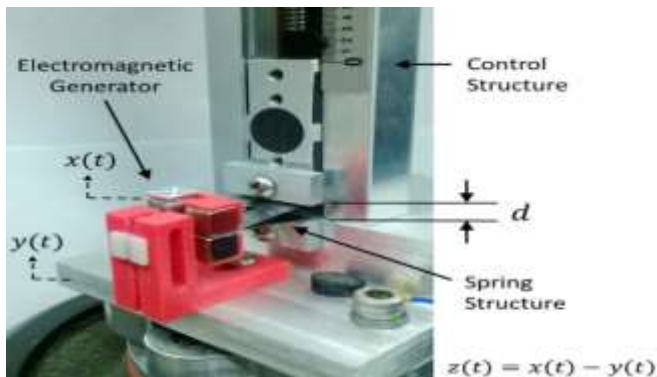


Fig. 1: Frequency tuneable EM energy harvester [51]

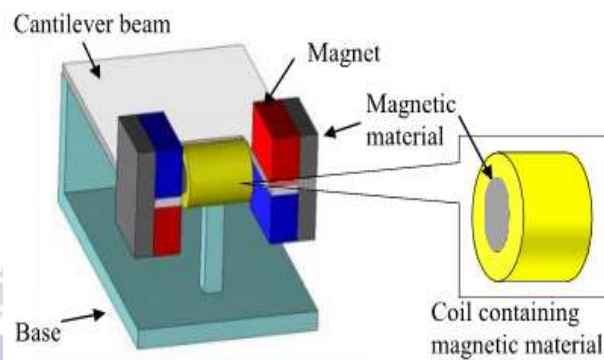


Fig. 2: Schematic of the EM harvester [52]

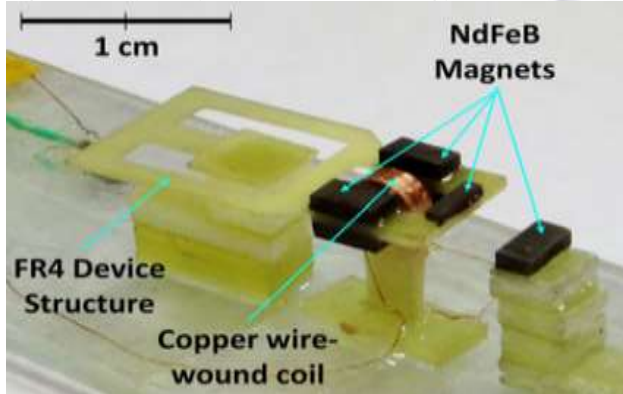


Fig. 3: Prototype of non-linear EM energy harvester [53]

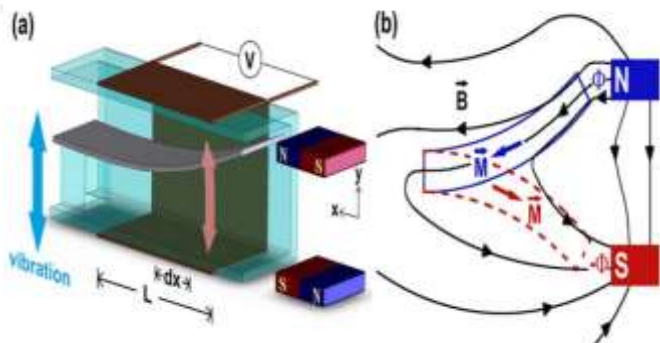


Fig. 4: (a) EH's schematic (b) with flux change [54]

A wideband VEMEH with a high-permeability cantilever beam was described by X. Xing et al. [54]. The gadget used a 46 mm x 8 mm x 0.254 mm high-permeability cantilever beam with a 44 mm x 32 mm x 40 mm solenoid. Fig. 4 shows two identical 22 mm x 13 mm x 2 mm anti-parallel Samarium-Cobalt (Sm. Co) rectangular magnets near the beam. The harvester, with a volume of 68.96 cm<sup>3</sup>, produced 74 mW of maximum power at 54 Hz and 0.57 g vibration level, resulting in 1.07 mW/cm<sup>3</sup> power

density. The device worked from 30 to 70 Hz with a 10 Hz bandwidth.

R. Paul and B. George [55] used a spherical flipping magnet to create a low-frequency VEMEH (Fig. 5). The 15-mm NdFeB spherical magnet was free to move inside a bobbin. Teflon bobbins with V-groves and 16 mm inner diameters were made vertically and horizontally. Both vertical and horizontal bobbins have 300 turns of 42 gauge copper wire windings with a coil resistance of 52.5

$\Omega$ . The device was tested from 0.25 to 3.5 Hz. The harvester's power as function of frequency plot showed a 1.5 Hz bandwidth. The device, measuring  $3.59 \text{ cm}^3$ ,

produced a power density of  $445 \text{ } \mu\text{W}/\text{cm}^3$  at 3.5 Hz vibration, with an open circuit  $V_{pp}$  output voltage of 3.5 V and an average power-out of 1.66 mW.

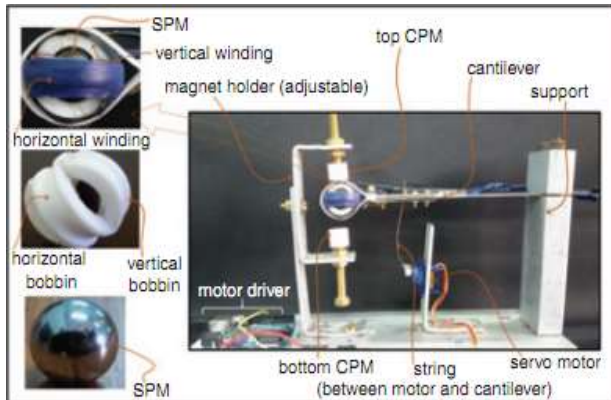


Fig. 5: Experimental setup and developed EH [55]

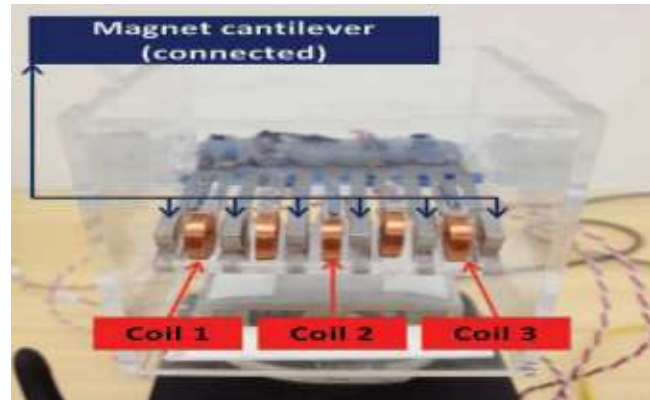


Fig. 6: Prototype of the developed VEMEH [56]

Jinkyoo Park et al. [56] reported a VEMEH that moves the coil and magnet in response to ambient vibrations. The gadget had 11 cantilevers, 6 of which had permanent magnets linked to their tips through magnet holders, and a set natural frequency of 6.8 Hz. The other 5 cantilevers with the same geometry and rigidity carry identical coils. The coil cantilever beams had varying tip masses, changing the natural frequency of each coil carrying cantilever from 7 Hz to 8.6 Hz and causing asynchronous movement in the harvester. The harvester was tested for low frequency (below 5 Hz) and mild acceleration vibrations. The gadget has 1.3 Hz bandwidth. During tests on Nong-Ro Bridge (Korea), adding tip weights to coil carrying cantilevers increased their frequency range to the bridge's resonance frequency (3 Hz) and generated  $30 \text{ } \mu\text{W}$  peak power.

M. S. M. Soliman et al. develop a wideband VEMEH [57]. The stator houses the harvesters' magnetic parts, while the translator handles mechanical suspension and coils. Fig. 7 shows a system with a cantilever beam ( $45.3 \text{ mm} \times 10 \text{ mm} \times 1.02 \text{ mm}$ ) bearing a seismic mass and a coil ( $160 \text{ } \mu\text{m}$ , 22 turns,  $1 \text{ cm}^2$ ) moving in a stationary magnetic field comprising four permanent magnets ( $1 \text{ cm} \times 1 \text{ cm} \times 0.3 \text{ cm}$ ). The device also has a slider and adjustable stopper on a track that adjusts the beam length and exhibits a wide range of the harvester's approved frequency. At 0.1 g and 90 Hz to 100 Hz, the device produces 19.5 mV. The harvester is projected to have 1.4 Hz bandwidth.

A wideband VEMEH is devised by M. S. M. Soliman et al. [57]. The magnetic parts of the harvesters are housed by the stator, whereas the mechanical suspension and coil arrangement is carried by the translator. The device depicted in Fig. 7 consisted of a cantilever beam ( $45.3 \text{ mm} \times 10 \text{ mm} \times 1.02 \text{ mm}$ ) carrying a seismic mass and a coil ( $160 \text{ } \mu\text{m}$ , 22 turns with an area of  $1 \text{ cm}^2$ ) movable in a surrounded stationary magnetic field constituted by four permanent magnets each one of size  $1 \text{ cm} \times 1 \text{ cm} \times 0.3 \text{ cm}$ . Moreover, the device carries a slider and an adjustable stopper movable along a track which varies the effective length of the beam and thus exhibits a wide band of the harvester's accepted frequency. The device functions at a constant acceleration level of 0.1 g within a frequency range of 90 Hz to 100 Hz, yielding a maximum voltage of 19.5 mV. The predicted frequency bandwidth of the designed harvester is 1.4 Hz.

Yang et al. [58] described a fixed-fixed beam VEMEH with three magnets and coils (Fig. 8). The harvester has three resonance frequencies: 369 Hz, 938 Hz, and 1184 Hz. Experimentally, the harvester is tested at 0.76 g vibration levels from 0 to 1.5 KHz. At 0.76 g and 369 Hz, the three series coils' maximum open circuit voltage is 0.2 mV. The first mode is reported to generate  $0.6 \text{ } \mu\text{W}$  of peak output power, while the second mode generates  $3.2 \text{ } \mu\text{W}$ . The voltage against frequency plot estimates the frequency bandwidth for the first mode of vibrations at 50 Hz and the second mode at 80 Hz.

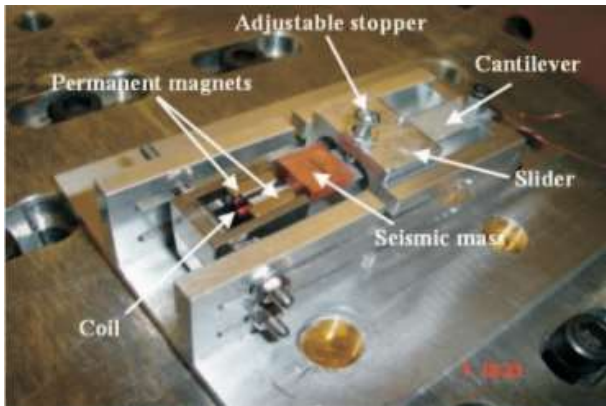


Fig. 7: Photograph of the fabricated EMEH [57]

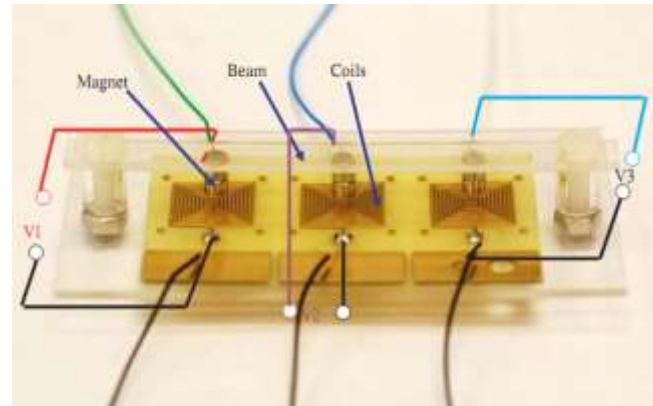


Fig. 8: Photograph of the reported VEMEH [58]

Sari et al. created a VEMEH with a fixed permanent magnet and 35 resonant frequency oscillating cantilevers to increase frequency bandwidth [59]. Coil-patterned parylene cantilevers of various lengths are illustrated in Fig. 9. To cover a wide range of frequencies, the harvester increases each cantilever's length by a modest amount. The coils generate voltage when the central block magnet moves. Experimentally tested, this 14 mm × 12.5 mm × 8 mm gadget generates 10 mV voltage from 4.2 kHz to 5 kHz operating frequencies. The output power against frequency plot estimates the harvester's frequency bandwidth at 300 Hz (3350-3650 Hz). The VEMEH is reported to generate 0.4 μW of power.

Liu et al. [60] reported a VEMEH with three multi-modal spring mass structures and a permanent magnet on the

fixed-fixed beam. Fig. 10 shows a VEMEH with three independent spring-mass components that vibrate during operation. In the harvester, folding springs sustain the shuttle mass carrying the planar aluminium spiral coil. The 1 cm x 0.8 cm x 0.04 cm micro-fabricated spring-mass structure was made using double side deep reactive ion etching (DRIE) on a silicon on insulator (SOI) wafer. During 1 g acceleration, the device's open circuit output voltage ranges from 0.01 mV to 0.13 mV, while the generated power ranges from  $0.303 \times 10^{-6} \mu\text{W}$  to  $16.012 \times 10^{-6} \mu\text{W}$ , resulting in a power density of  $0.010 \times 10^{-3} \mu\text{W}/\text{cm}^3$  to  $0.500 \times 10^{-3} \mu\text{W}/\text{cm}^3$ . Maximum frequency bandwidth determined from voltage vs. frequency plot is 10 Hz.

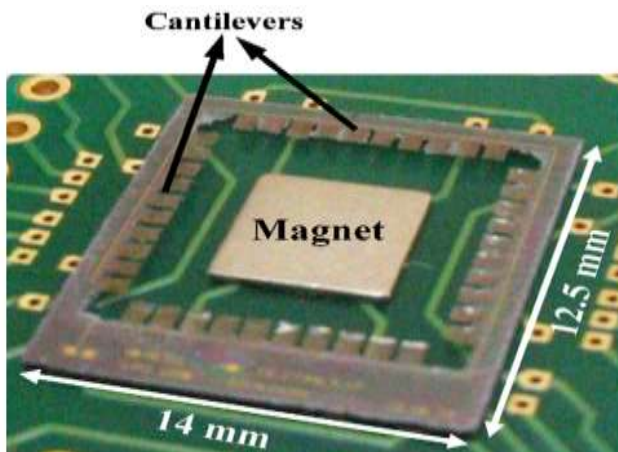


Fig. 9: Photograph of the developed VEMEH [59]

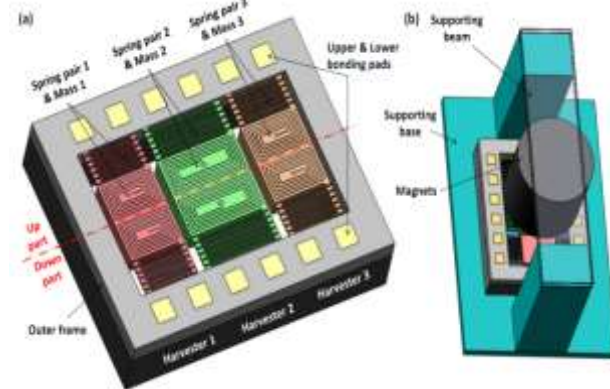


Fig. 10: (a) 3D drawing (b) Reported VEMEH [60]

Tao et al. [61] reported a two-subsystem, multimodal (2DOF) VEMEH. Primary subsystem creates power, while accessory subsystem tunes harvester frequency. Fig. 11

shows the outer circular spring supporting primary mass. The external oscillations jiggle this main mass relative to the fixed magnet, generating voltage across the coil

terminals. The 1.45 cm × 1.45 cm × 0.043 cm gadget, tested at 0.12 g acceleration, produced 3.6 mV at 326 Hz and 6.5 mV at 391 Hz resonant frequencies. The maximal output power of the device is 0.96 nW, whereas the normalised power density is 2.75 × 10<sup>-2</sup> W/cm<sup>3</sup>/g. The device's frequency upswep is 300–420 Hz, and the voltage against frequency plot estimated a 2 Hz bandwidth.

Fan et al. [62] constructed a monostable very low frequency (less than 10 Hz) VEMEH with a tube wrapped in coil, two fixed magnets at the tube ends, and a magnet spring resonator within. As shown in Fig. 12(a), the central moveable magnet attracts both end magnets,

causing spring softening and lowering the operating frequency. Experiments reveal that the harvester generated 1.15 mW of electricity at 0.8 g acceleration and 9 Hz frequency under sinusoidal excitation. The frequency vs. voltage figure estimates the device's frequency bandwidth at 2 Hz (9–11 Hz). The harvester charged a 47 μF capacitor from 0 to 4 V in 2 seconds when activated by hand shaking. In treadmill experiments, the created VEMEH produced roughly 0.5 mW of power while walking (4 to 6 km/hr) when fastened on the leg in vertical position (Fig. 12(b)). However, the prototype generated 0.7 mW power when fastened on the leg in parallel and tested at 7–9 km/hr.

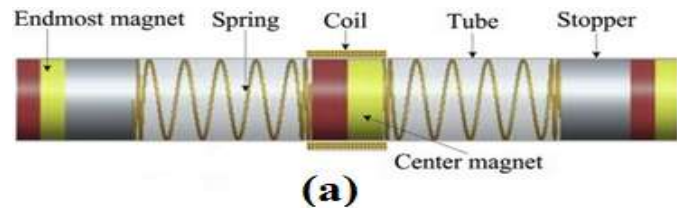
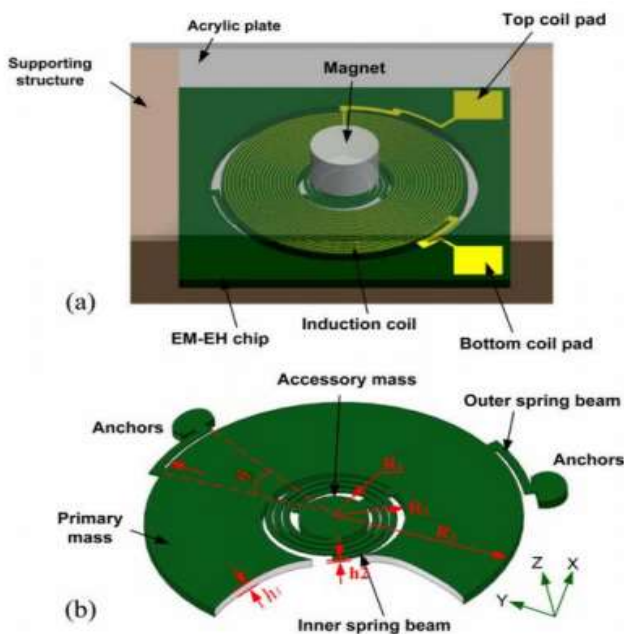


Fig. 11: (a) VEMEH's schematic , (b) Trimetric view [61] Fig. 12: (a). VEMEH's schematic, (b). Developed prototype attached to leg [62]

III. (B) NON-RESONANT VEMEHS

Independent of a given resonant frequency, a non-resonant VEMEH uses Faraday's law of induction to convert mechanical energy into electrical energy. Usually in non-resonant harvesters, the magnet and coil are not adjusted to oscillate at a specific resonant frequency. Rather, they are meant to change in respect to one another depending on outside vibrations or other mechanical forces.

A VEMEH based on non-resonant and wide-band ambient vibrations was designed by Iman Shahosseini et al. [63]. Fig. 13 shows the gadget. Using a shaking table,

prototypes (4 mm length, 6 mm thickness, 60 Ω) and 2 mm length, 5 mm thickness, 25 Ω coils were tested for vibration. The vertical movement of magnets relative to stationary coils generated voltage. When tested outside resonance frequency, the EMEH increased power from 30 μW to 2.2 mW at frequencies from 3 to 12 Hz at 1 mm vibration amplitude.

Tzeno Galchev et al. designed a VEMEH to scavenge non-periodic low-frequency vibrations [64]. The coil has a 3.175 mm diameter, 4.75 mm thick cylindrical magnet on top. A coil of 2 mm diameter, 3.175 mm length, and 240 Ω resistance was employed in the harvester. A grade N42,

NdFeB, magnet (2.4 mm x 4.76 mm) was connected to a spring on top of a plastic spacer (1mm x 1mm x 0.5 mm) to form the frequency enhanced generator (FIG) spring assembly. A 3.75 cm<sup>3</sup> parametric frequency-increased generator (PFIG) with an internal volume of 2.12 cm<sup>3</sup> was

tested at 1 g acceleration and 10 Hz frequency, generating a maximum of 163 μW and an average of 13.6 μW (Fig. 14). The device could function at 65 Hz, according to reports.

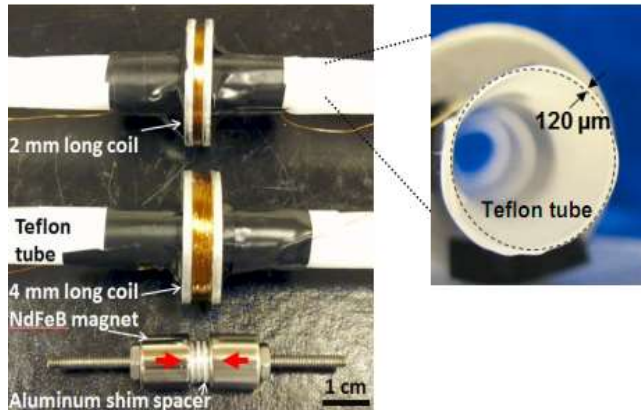


Fig. 13: Developed prototype of harvester [63]

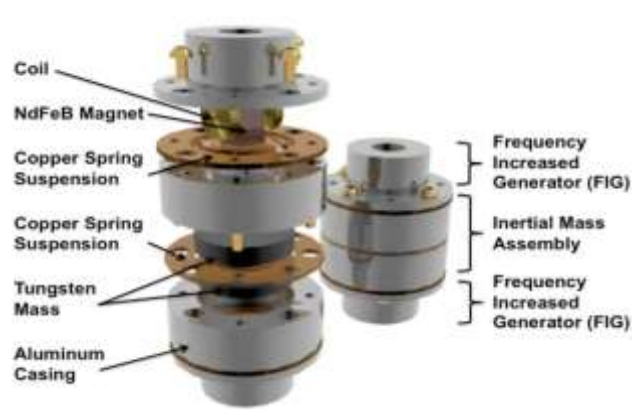


Fig. 14: Reported micro power generator [64]

Jeongjin Yeo et al. [65] designed multi-dimensional harvesters to handle various ambient vibrations. Fig. 15 shows coil solenoids coiled externally on both harvesters' housings. The prototypes were tested from 3 to 100 Hz. The cylindrical harvester with a bandwidth of 25 Hz, estimated from voltage vs. frequency graph, had a maximum RMS voltage of 5.7 V at 30 Hz and 19.03 mW highest power, while the doughnut-shaped harvester had 5.4 V at 9 Hz and 2 Hz bandwidth.

wide sealed chamber (hole) in the centre and 12 layers of 10-turn planar copper coils. Vibrations allow a 3 mm x 4 mm Neodymium (NdFeB) cylindrical magnet in the middle chamber to move up and down. Additionally, acrylic sheets cover the container. Drilling small holes in the acrylic cover plate reduced harvester air damping. The device had 2.7 cm<sup>3</sup> volume and produced 9 mV voltage from vibration at 1.9 g acceleration at 40-90 Hz. The harvester operated within a 10-300 Hz frequency range and generated 0.4 μW peak power with a 40-80 Hz bandwidth.

Bin Yang et al. [66] built a non-resonant, wide-band frequency harvester (Fig. 16). Harvester was made by stacking five 2 mm thick FR4 substrates with a 4 mm

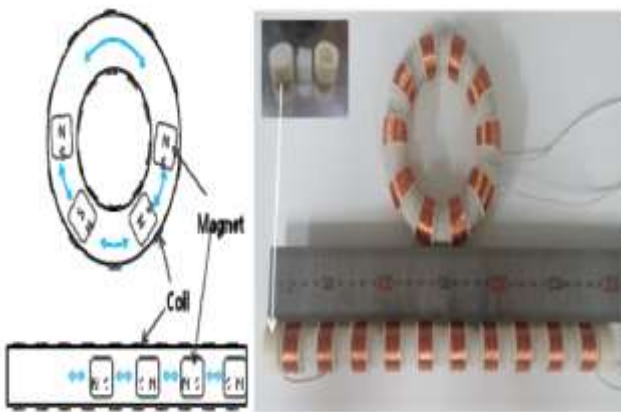


Fig. 15: Developed circular magnet type VEMEHs [65]

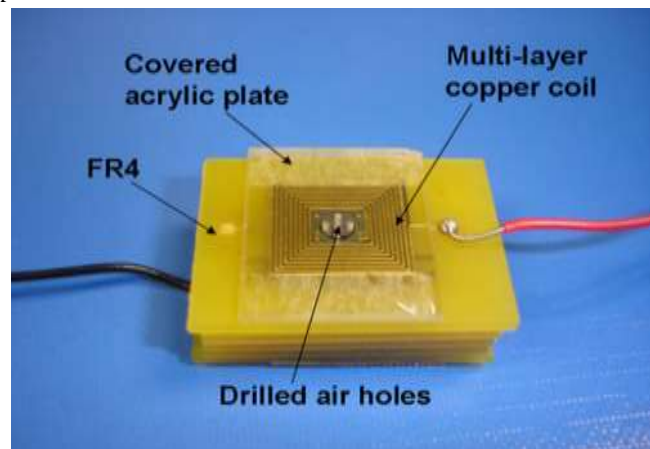


Fig. 16: Fabricated wide band energy harvester [66]

S. Bradai et al. constructed Fig. 17's wide-frequency non-linear VEMEH [67]. The designed harvester operates at 10-60 Hz with a 20-Hz bandwidth. The non-linear wide-band VEMEH is evaluated and found to harvest 1.5 times more energy than a simple EM harvester at 20-35 Hz, 2 mm excitation amplitude, and 33  $\Omega$  load resistance. Fan et al. [68] created a 2-DoF VEMEH. A cylindrical housing with extra coils (1-DoF VEMEH) is modified to make the harvester. The primary VEMEH and housing magnetically join to create the 2-DoF VEMEH. Thus, this

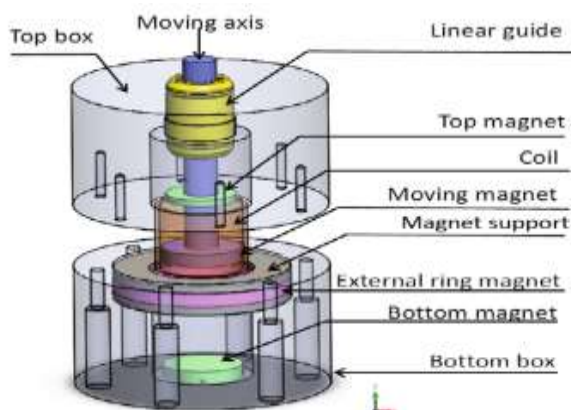


Fig. 17: Proposed VEMEH's schematic [67]

Zorlu et al. created a small non-resonant VEMEH for low-frequency, low-acceleration energy generation [69]. The developed device had a 2 mm x 2 mm cantilever beam, a NdFeB permanent magnet (2.5 mm x 0.5 mm) attached to an oscillator's shaker stage, a 40-layer dual-level micro machined planar coil, and a polystyrene film mechanical barrier arm joined to the magnet's upper surface. Figure 19 shows the energy harvester, with a 0.12 cm<sup>3</sup> volume and 21.5  $\Omega$  coil resistance. At 0.8 g acceleration and 10 Hz frequency, the harvester achieves 1.44 mV RMS load voltage, 24 nW output power, and 200 nW/cm<sup>3</sup> power density.

M. A. Halim et al. [70] created a non-resonant frequency up-converted broad band VEMEH to generate power from human movement. The VEMEH in Fig. 20(b) has a

magnetic suspension may generate electricity from extremely low frequency vibrations. Experimentally, the 2-DOF VEMEH produced 2.58 mW peak power at 7.5 Hz with 0.5 g amplitude, which was better than the 1-DoF's 1.86 mW. Experimentally testing the harvester for 5-25 Hz frequency gap, the power vs. frequency graph estimated the frequency bandwidth at 2 Hz (6.5-8.5 Hz). The 2-DOF VEMEH had a 9.1 Hz operational bandwidth, compared to 3.6 Hz for the 1<sup>st</sup> type. Fig. 18 shows both EH prototypes.

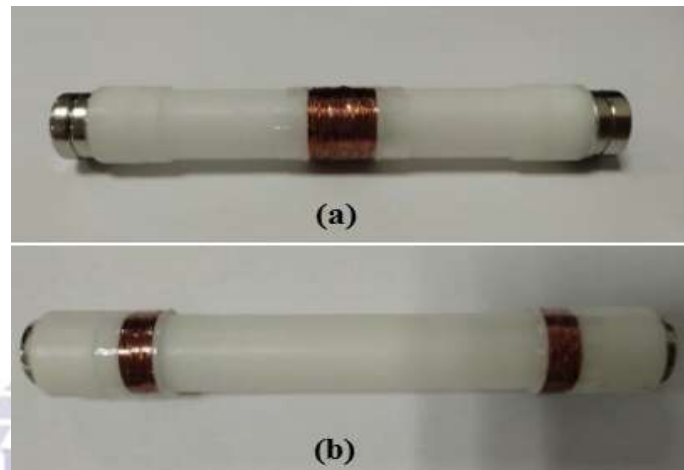


Fig. 18: Wide-band VEMEH (a) 1-DoF (b) 2-DoF [68]

hollow acrylic cylinder, two helical steel springs, two acrylic end caps, two 200-turn copper wrapped coils, two permanent magnets (NdFeB), and a non-metallic ball. Using an external excitation of 1.53 g, 1.83 g, and 2.04 g produced RMS open circuit voltages of 33.7 mV, 40.1 mV, and 45.3 mV for the working frequency range of 14 Hz to 22 Hz in a 6.75 cm<sup>3</sup> device. The harvester was tested at 12-60 Hz and expected to have an 8-Hz bandwidth. However, the device exhibited irregular or arbitrary voltage outputs between 23 Hz and 39 Hz, showing a deteriorating trend in performance. Due to the ball's non-prominent movement, which prevented it from hitting the magnets, the gadget produced very little voltage at 40-60 Hz.

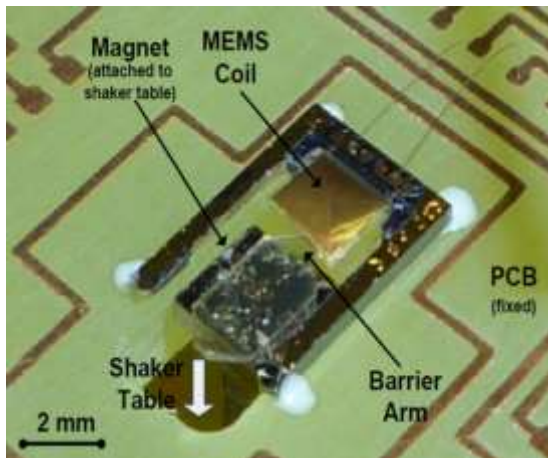


Fig. 19: Photograph of non-resonant VEMEH [69]

Li et al. [71] reported a non-resonant VEMEH for automobile key remote controllers. Fig. 21 shows a cylindrical block magnet that could freely travel inside a 20-mm round chamber. Both cavity sides were covered with PCB-fabricated multilayer copper planar coils. The copper coils and magnet's movement generated voltage across the terminals. The 4-layer planar copper coil was made utilising FR-4 PCB technology with 100  $\mu\text{m}$  wire width and 35  $\mu\text{m}$  thick turns. At 100 mm vibration magnitude and 3 Hz frequency, a 3.1-mm harvester vibrated with a z-axis polarised magnet produced 1.1 V of open circuit voltage. Also, increasing magnet size with bigger radius increased coil induced voltage.

Bowers et al. [72] designed a VEMEH with a spherical chamber that houses the freely moveable NdFeB and captured energy from human motion. The casing was wrapped with a 34-gauge copper coil to create the wound coil. Fig. 22 shows prototype-1 and prototype-2. Running prototypes produce more output voltage than walking prototypes. During testing, prototype-2 (held in trouser pocket) produced higher output voltage (680 mV) and greater power density (0.5  $\text{mW}/\text{cm}^3$ ) than prototype-1 (350 mV, 0.12  $\text{mW}/\text{cm}^3$ ). The gadget was tested for 1-10 Hz low-frequency operations.

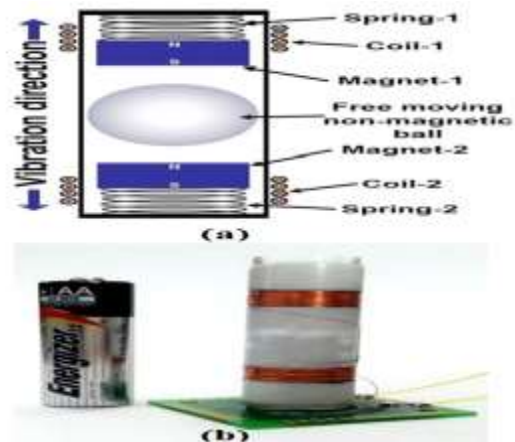


Fig. 20: (a) Schematic (b) Developed VEMEH [70]

Han et al. [73] made a spring-less cubic VEMEH that converts three-axis vibration into electrical power. Fig. 23 shows how copper planar coils and a folded substrate make a cube. The cube contained a permanent NdFeB magnet that can move freely without spring support, allowing the device to harvest in all directions. The 1  $\text{cm}^3$  harvester operated from 20 to 100 Hz. The harvester's frequency bandwidth is estimated at 3 Hz (25-28 Hz) from voltage versus frequency. The gadget generated a maximum voltage of 3.82 mV at 26.87 Hz with a peak output of 0.75  $\mu\text{W}$  and a power density of 0.75  $\mu\text{W}/\text{cm}^3$  when operated at 0.5 g acceleration.

Erol Kurt et al. [74] reported another non-resonant VEMEH using changing magnetic induction at the coil's core with two stable magnets and a spacer. The impact vibrations affect the spacer's air-gap, generating voltage. Fig. 24 shows the prototype and experiment setup. The harvester generated 2.41 mV RMS at 60 Hz and 1 mm displacement. The output power was 17  $\mu\text{W}$  at the same vibration level, resulting in 0.358  $\mu\text{W}/\text{cm}^3$  power density. Power harvesting was possible from 2 Hz to 1.5 kHz with the gadget.

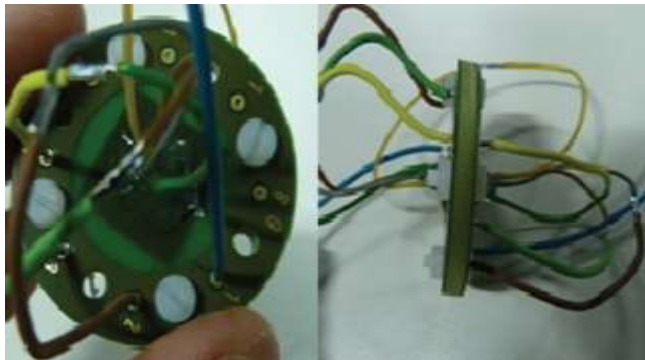


Fig. 21: A non-resonant VEMEH developed [71]



Fig. 22: VEMEH: (a) Prototype-1, (b) Prototype-2 [72]

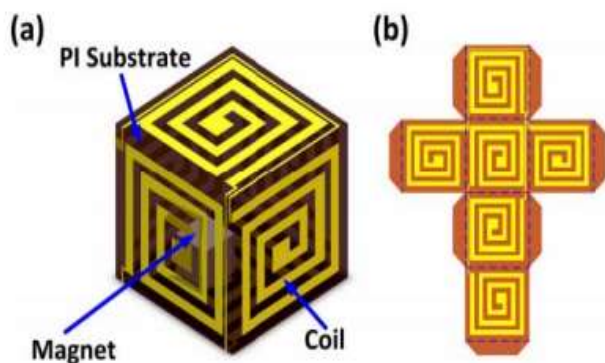


Fig. 23: VEMEH: (a) 3D drawing (b) Planar layout [73]



Fig. 24: A non-resonant VEMEH developed [74]

Y. Shen and K. Lu [75] built a non-resonant VEMEH with a cylindrical steel frame to increase flux and harvester power density and two identically polarised magnets facing each other. The harvester in Fig. 25 has a  $31.01 \text{ cm}^3$  volume. With the incidence vibration, a wound coil around a teflon portion moved freely inside the steel frame, producing output voltage. The energy harvester produced  $23.2 \text{ mW}$  power at  $3.25 \text{ g}$  and  $4.5 \text{ Hz}$  vibrations, resulting in  $748 \mu\text{W}/\text{cm}^3$  power density.

Zhang and Su [76] created another non-resonant VEMEH using magnetic springs to gather human motion energy. A non-magnetic shell, six coils of various diameters, two circular and two cylindrical permanent magnets made up the harvester. The travelling magnet was repelled by the two magnets' identical magnetisation. This force created a magnetic spring between the magnets. The developed harvester in hand motion is depicted in Fig. 26. The VEMEH was tested at various body motions and frequencies, generating  $2.2 \text{ V}$  voltage and  $0.024 \text{ W}/\text{mm}^3$  power density at  $6 \text{ Hz}$ .

K. Kecik and E. Stezycka [77] constructed a 2-DoF VEMEH to gather energy between primary and secondary

resonance locations. The harvester has two 20-mm-diameter, 30-mm-tall permanent magnets,  $A_1$  and  $A_2$ .  $A_1$  and  $A_2$  might move freely due to the repulsion of the stationary magnets  $B_1$  and  $B_2$ . The fixed end magnets were  $20 \text{ mm} \times 5 \text{ mm}$ . All the magnets were gathered in a non-magnetic PVC hollow cylinder and wound in 12740 turns around a  $0.14 \text{ mm}$  copper wire in a  $21 \text{ mm}$  inner diameter tube. Moving magnets were affected by magnetic forces from the device's upper and lower magnets. Two bumpers inside the tube reduce magnetic impacts. The movable magnet's relative movement to the stationary coil caused a time-varying magnetic flux and an electromotive force. The fixed and moveable magnets' repulsive force caused non-linearity and expanded the resonance frequency spots. The EH in Fig. 27 was experimentally tested to produce  $0.2 \text{ W}$  of power with a bandwidth of  $9.55\text{--}19 \text{ Hz}$ .

P. Holm et al. [78] reported a magnetic dumbbell-based high-power VEMEH, Fig. 28. This device has a tube with two stationary magnets and two coils and a buoyant, freely moving dumbbell assembly with two magnets. Evaluation of the device showed peak power of  $1.04 \text{ mW}$

at 8.5 Hz and 0.87 g acceleration, resulting in  $50 \mu\text{W}/\text{cm}^3$



Fig. 25: A non-resonant VEMEH developed [75]

power density within the 4-20 Hz frequency limit.

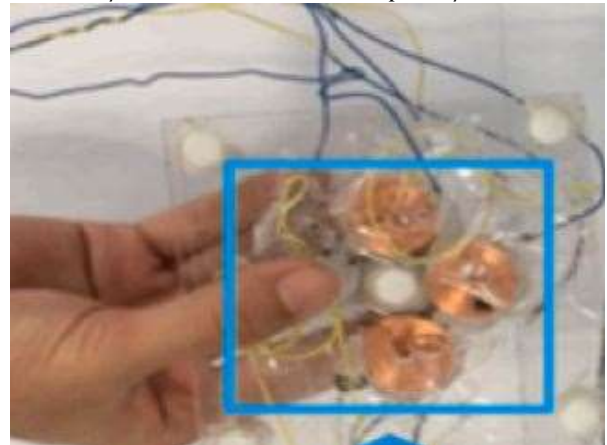


Fig. 26: Developed non-resonant VEMEH [76]

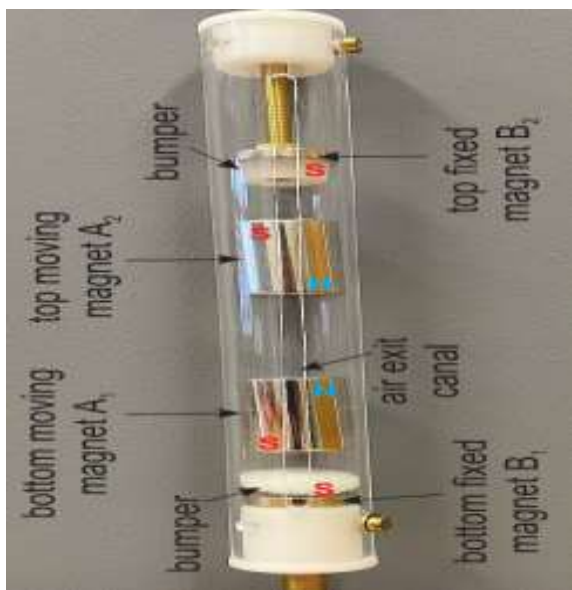


Fig. 27 Developed non-resonant VEMEH [77]



Fig. 28 Developed non-resonant VEMEH [78]

Magnetic levitation-based VEMEH by Jeong et al. [79] used a 3D-printed bobbin and housing unit. Fig. 29 shows a primary magnet, secondary magnet, and copper-wound coil. The mutually attracting force of two magnets created a magnetic spring, increasing operation frequency. A VEMEH with  $83.03 \text{ cm}^3$  volume generated 4.28 mW power, resulting in a power density of  $51.56 \mu\text{W}/\text{cm}^3$ .

Li. G. et al. [80] designed a composite core and magnetic fluid multi coil VEMEH to improve output and operating

frequency range. The constructed energy harvester outperforms non-magnetic liquid harvesters by 29% in power output. The operational frequency range has also increased. Developed multi-core magnetic fluid energy harvester produces  $134.26 \mu\text{W}/\text{cm}^3\text{g}^2$  normalised power density. The vibration frequency was 6-15 Hz. Fig. 30 shows the multi-core VEMEH.



Fig. 29 Developed non-resonant VEMEH [79]

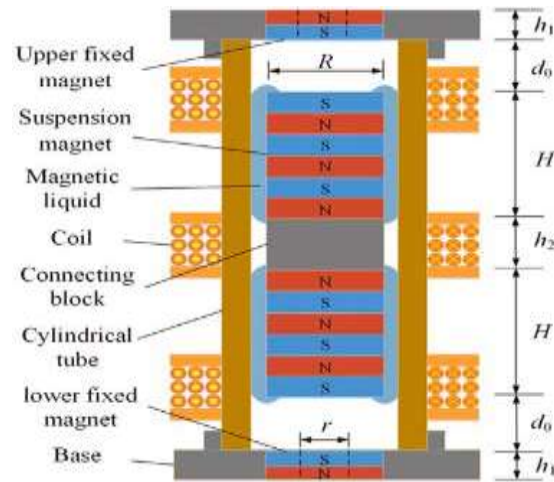


Fig. 30 Developed multi core VEMEH [80]

Lorenzo et al. [81] created a wideband 3D-printed Vibration Energy Micro-Electro-Mechanical Harvester (VEMEH) with two stacked ortho-planar springs. The core pivot-linked moving parts have magnets attached. Half of the magnetic field was orientated upward and half downward in the magnet array, generating a balanced and alternating magnetic field distribution. A robust frame held a copper-wound coil and ortho-planar springs. Device bandwidth was tested between 10 and 30 Hz. The max output power at 15.1 Hz is 5 mW, resulting in a normalised power density of  $2.2 \mu\text{W}/\text{cm}^3 \text{ (m/s}^2\text{)}^2$ . The gadget is in Fig. 31.



Fig 31: Developed VEMEH [81]

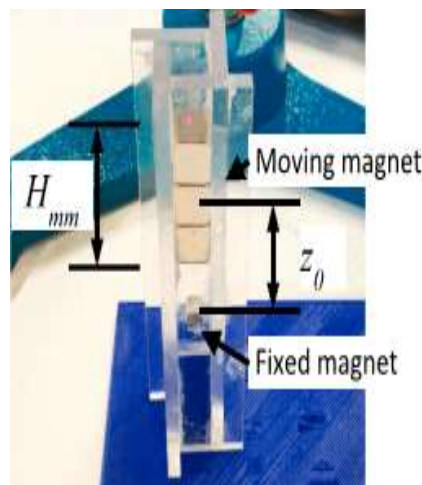


Fig. 32: Developed VEMEH [82]



Fig. 33: Fabricated VEMEH [83]

Wang L. et al. [83] built a low-frequency VEMEH with a compact flexure guiding structure to reduce housing and magnet friction. Flexure structure reduced coil and magnet space, increasing induced emf. The  $123 \text{ cm}^3$

(Fig. 32) Royo S. et al. [82] presented a low-frequency VEMEH prototype combining magnetic levitation and a ferrite magnet to capture energy from vertical vibrations. In the centre was a 350-turn coil facing the moveable magnet's top. The stationary and mobile magnets used four small ferrite magnets and two NdFeB magnets. Low-frequency vibrations between 1 and 3 Hz are designed into the harvester. The gadget had a capacity of around  $600 \text{ cm}^3$ . The greatest output power at 1.7 Hz and 0.5 g was 4.38 mW.

VEMEH was tested at 19.5 Hz and 0.1 g vibration, resulting in 6.08 V voltage and 4.02 mW output power. Normalised power density measured was  $3.28 \text{ mW}/\text{cm}^3\text{g}^2$ . Fig. 33 shows the fabricated VEMEH.

For wearable applications targeting low-frequency human body vibrations, P. Xiaugi et al. [84] developed VEMEH. A permanent magnet at the top of a tumbler converts human motion into electricity. The device works for 1-5 Hz human body excitations. The developed device has a capacity of 30 cm<sup>3</sup>. The developed EH produced 0.86 mW of power at 4 Hz and 12 km/hr, resulting in 28.67 μW/cm<sup>3</sup> power density. The designed harvester measured 10.75 μW/g of power per unit acceleration. Fig. 34 shows the energy harvesting design.

A wide-band VEMEH was developed by R. Murugesan et al. [85] using magnetic solenoid pendulum arrays. Each

array has two pendulums, one with a permanent magnet and the other a solenoid coil. Supports on vibrating hosts carry all their pendulums. External vibrations caused the entire pendulum and array assembly to oscillate, creating energy. Unlike individual magnet-solenoid pendulum arrays, the harvester array captured sustained energy across a broad frequency spectrum in testing. Compared to a solitary harvester, the power-out is 200 μW and the bandwidth has increased by 45.57%. The recorded power density is 128 μW/cm<sup>3</sup>. Fig. 35 shows the wide-band VEMEH pendulum array schematic.

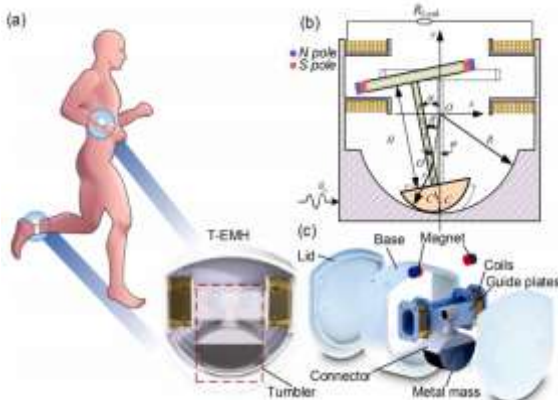
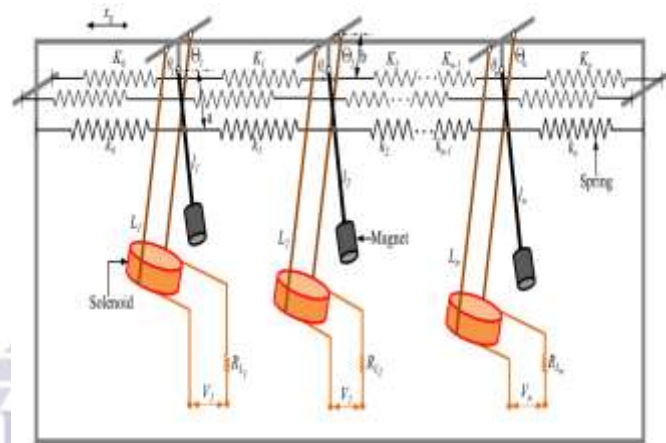


Fig. 34: Developed non-resonant VEMEH [84]



			(Hz)			(μW)	<sup>3)</sup>		n (μW/cm <sup>3</sup> g)	
Resonant	1600 <sup>a</sup>	0.2	32 - 85	5	260	340	0.21	1700	1.05	[51]
	-	-	20 - 160	140	-	100	-	-	-	[52]
	13.31 <sup>b</sup>	1.5	10-50	8	150	19.3	1.45	12.86	0.96	[53]
	68.96	0.57	30-70	10	650	74000	1073	129824	1877	[54]
	3.59	-	0.25 - 3.5	1.5	3500	1660	445	-	-	[55]
	-	-	0.5 - 5	1.3	-	30	-	-	-	[56]
	675 <sup>a</sup>	0.1	90 - 100	1.4	19.5	-	-	-	-	[57]
	3.4 <sup>a</sup>	0.75	0-1500	80	-	3.2	0.941	4.26	1.24	[58]
	1.4	-	4200 - 5000	300	10	0.4	0.286	-	5.72 x 10 <sup>-3</sup>	[59]
	0.032	1	189 - 662	10	0.01 to 0.13	16.012 x 10 <sup>-6</sup>	0.50 x 10 <sup>3</sup>	16.012 x 10 <sup>-6</sup>	0.500 x 10 <sup>3</sup>	[60]
	0.091	0.12	300-420	2	3.6 & 6.5	0.00096	3.30 x 10 <sup>3</sup>	0.008	27.5 x 10 <sup>3</sup>	[61]
	12.19 <sup>b</sup>	0.8	5-25	2	-	1150	94.33	1437.5	117.91	[62]
Non-resonant	11.37 <sup>a</sup>	5.67 <sup>c</sup>	3 - 12	9	300	2200	193.7	388	34	[63]
	3.75	1	10 - 65	-	100	13.6	3.63	13.6	3.63	[64]
	95.56	-	3-100	25	5700	19030	199	-	-	[65]
	2.7	1.9	10-300	40	9	0.4	0.148	0.21	0.0778	[66]
	-	-	10-60	20	370	-	-	-	-	[67]
	-	0.5	5-25	2	-	2580	-	5160	-	[68]
	0.12	0.8	10	-	1.44	0.024	0.2	12.5	0.250	[69]
	6.75	2	12-60	8	45.4	-	-	-	-	[70]
	0.975 <sup>a</sup>	3.62 <sup>c</sup>	3	-	1100	-	-	-	-	[71]
	4	-	1 - 10	-	680	2000 <sup>b</sup>	500	-	-	[72]
	1	0.5	20 - 100	3	3.62	0.75	0.75	1.5	1.5	[73]
	47.48 <sup>b</sup>	-	2-1500	60	2.41	17	0.358	-	-	[74]
	31.01	3.25	-	4.5	-	23200	748	7138	230	[75]
	-	-	-	6	2200	-	24	-	-	[76]
	-	-	9.5-19	-	-	200	-	-	-	[77]
	20.8 <sup>b</sup>	0.87	4-20	16	-	1040	50	1195	57.47	[78]
	83.03	-	-	-	-	4280	51.56	-	-	[79]
	-	-	6-15	9	-	-	-	-	134.26	[80]
	-	-	10-30	20	-	5000	-	-	-	[81]
	600	0.5	1-3	2	-	4380	7.3	8760	14.6	[82]
123	0.1	19.5	-	6080	4020	32.68	60800	328	[83]	
30	-	1-5	4	-	860	28.67	10.75	-	[84]	
1.56 <sup>b</sup>	-	-	-	-	200	128	-	-	[85]	

<sup>a</sup>Estimated from dimensions provided

<sup>b</sup>Calculated by given power density

<sup>c</sup>Calculated by  $a=y(2\pi f)^2$

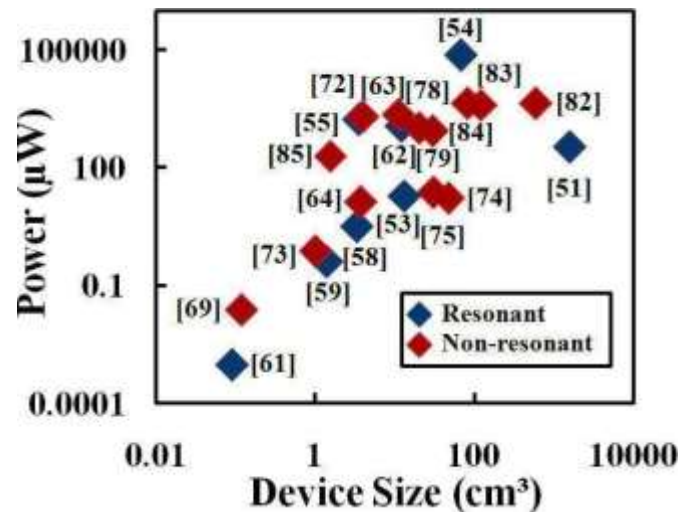
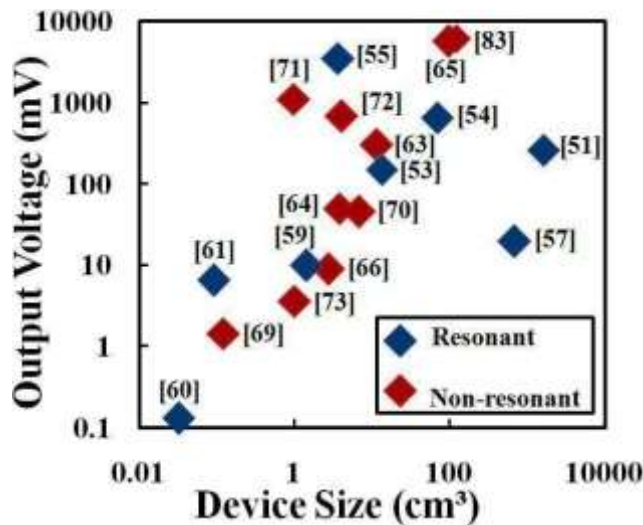


Fig. 36: Voltage vs. device size of the reported VEMEHs Fig. 37: Power vs. device size of VEMEHs

The comparison on the basis of power density and acceleration is shown in Fig. 38. The device produced in [54] which is resonant type is offering the maximum power density of 1073  $\mu\text{W}/\text{cm}^3$ , whereas the lowest

power density of  $0.500 \times 10^{-3} \mu\text{W}/\text{cm}^3$  was reported by the device developed in [60]. Overall, the power densities of resonant-type VEMEHs surpassed that of non-resonant type VEMEHs.

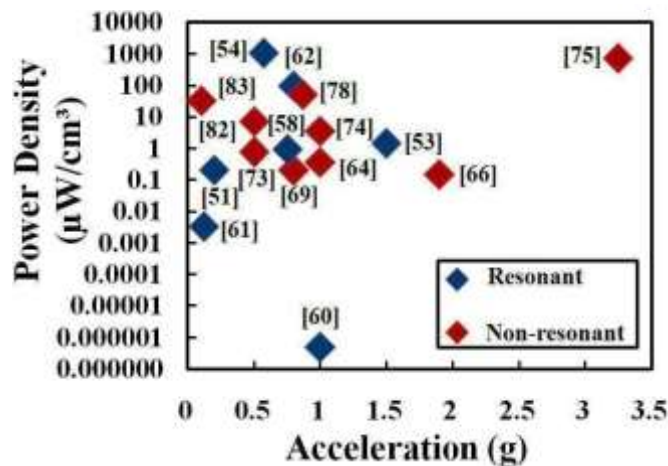


Fig. 38: Power densities vs. acceleration of the VEMEHs

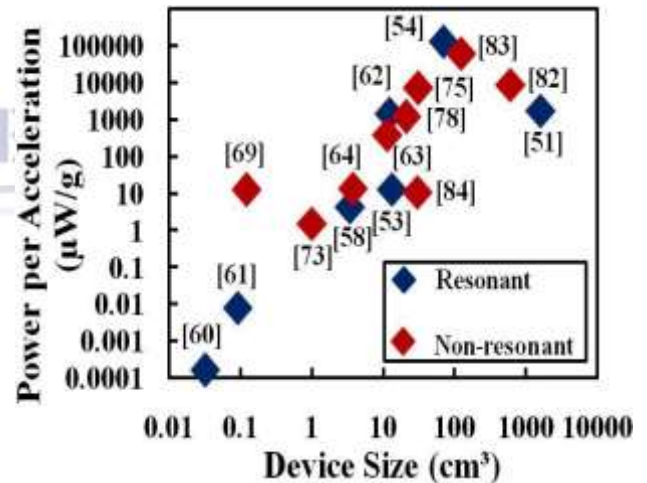


Fig. 39: Power/acceleration vs. device size

Fig. 39 compares acceleration power to gadget size. The resonant harvester mentioned in [54] offers the maximum power per acceleration at 129824  $\mu\text{W}/\text{g}$ . The harvester has the lowest power per acceleration at  $16.012 \times 10^{-6} \mu\text{W}/\text{g}$  [60]. In addition, Fig. 39 shows that resonance-based designs are more efficient in certain operating conditions because their power output per unit acceleration is higher. Cantilever beam arrangement or springs in such resonant devices increase power production at reduced acceleration. Non-resonant

VEMEHs need more acceleration amplitude to vibrate the harvesting device.

The comparison on the basis of the frequency bandwidth offered by each energy harvesting device and the power-out is illustrated in Fig. 40. The highest operating band of 300 is offered by the wide band VEMEH reported in ref [59] but the value of power obtained is only 0.4  $\mu\text{W}$ . The device's exceptionally wide frequency bandwidth is achieved through an array of 35 cantilevers, each oscillating at a different resonant frequency. This design results in a broader overall frequency range compared to

other reported VEMEHs, although its power output is lower than that of many other devices. The lowest value of frequency bandwidth which is 1.3 Hz is offered by the device presented in [56], however the peak power achieved from this device is 30  $\mu\text{W}$ . The power as

function of frequency bandwidth plot shows that on average the non-resonant VEMEHs are having wider frequency bandwidth as compare to the resonant VEMEHs.

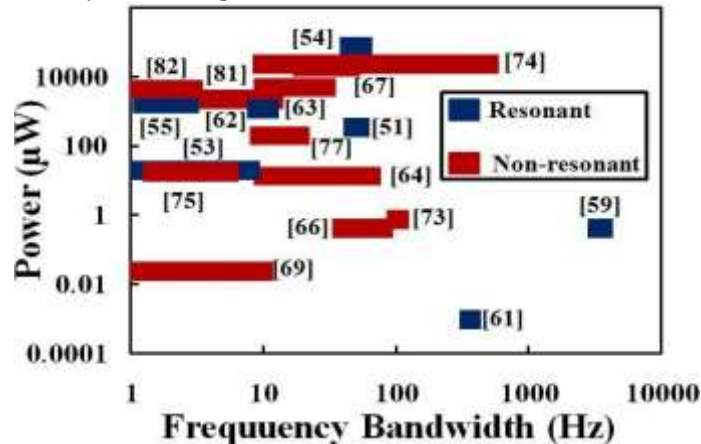


Fig. 40: Power output of the reported VEMEHs in comparison to frequency bandwidth

#### IV. VIBRATION ELECTROSTATIC ENERGY HARVESTER (VESEHs)

Energy harvesters based on the electrostatic conversion technique use a variable capacitor configuration, where relative movement between two plates generates electrical charges. An electrostatic or electret-based energy harvesting system generates electricity by the change in capacitance between two parallel plates. This energy harvester is one of a kind because it uses an electret, which is a permanent surface voltage source that may be used negatively or positively, to generate voltage. Many electrostatic MEMS energy harvesters have been proposed and fabricated to power remote wireless sensor nodes. A few of these developed harvesters are discussed and compared in the coming section based on their size, resonance frequency, output power, and power densities.

##### IV. (A) RESONANT VESEH

By means of a variable capacitor, a mass-spring system, and resonance, a resonant VESEH generates electrical energy from ambient vibrations, therefore augmenting the relative movement between the capacitor plates. The mass-spring system oscillates with rather larger amplitude when ambient vibrations coincide with the resonance frequency. This increased motion produces relative movement of the capacitor plates, therefore changing the capacitance. The voltage across the capacitor simultaneously changes with changing capacitance. Later

on, this voltage change is used to transfer energy to a load.

Powering the wireless sensor nodes and to come up with the energy requirements, a resonant electrostatic based EH has been produced by Jacopo Iannacci et al. [86] which converts ambient vibrations into useful power. The harvester shown in Fig. 41 has dimensions of 0.15 cm x 0.15 cm x 0.5 cm and was capable of converting in and out of plane excitations. The structure has been tested to have resonant frequency in 10-12 kHz limit and capable of converting ambient vibrations into power levels of  $\mu\text{W}$ . A high-performance ESEH for tyre pressure monitoring was presented by M. Renaud et al. [87]. The harvester, measuring 1 cm<sup>3</sup>, may power a tire pressure monitoring gadget. At 2.9 g vibration level, this gadget generated 160  $\mu\text{W}$  power from sinusoidal vibrations. The developed ESEH shown in Fig. 42. When aroused with vibrations like those of a moving tire, it generated 10-50  $\mu\text{W}$  of power.

Increasing proof mass and operational frequency has always had limits. M. E. Kiziroglou et al. [88] used a free-rolling proof mass to solve this. The variable capacitor's stationary plate in the proposed ESEH is made of electrodes and covered by a small dielectric. The gadget in Fig. 43 is proposed. A rolling rod-shaped metal cylinder is the counter electrode. The variable capacitor fluctuates because the cylinder and electrode make and break contact. Rolling a 0.75mm steel rod over strip capacitors

yielded 2.4 voltage gain. Small frequency and strong amplitude excitations suit the proposed device.

In many applications, energy harvested must be stored for periods without external vibration and wireless sensor nodes must always communicate data. A compact ESEH and Li-Ion micro battery presented by Erick O. Torres et

al. [89] met this criterion. Fig. 44 shows the proposed energy harvester design. The device was tested to use 570 pJ energy each cycle with 15 μs episodes, resulting in 38 μW average power-out. Using a Li-Ion battery to precharge the capacitor and store gathered energy starts the gadget.

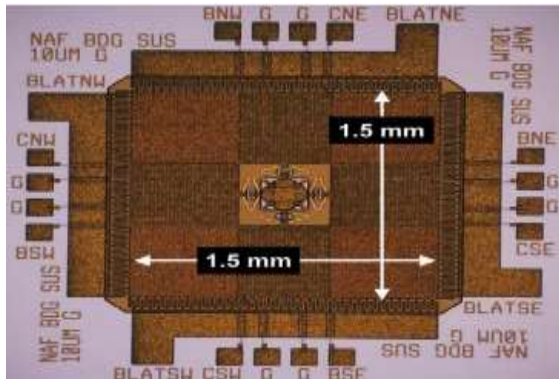


Fig. 41: Microphotograph of proposed VESEH [86]



Fig. 42: Proposed Energy Harvester [87]

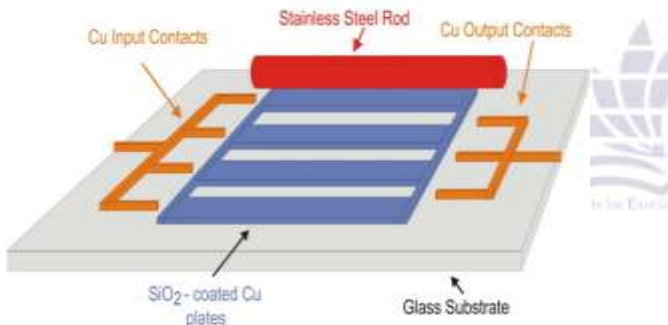


Fig. 43: Schematic of the rolling rod ESEH [88]

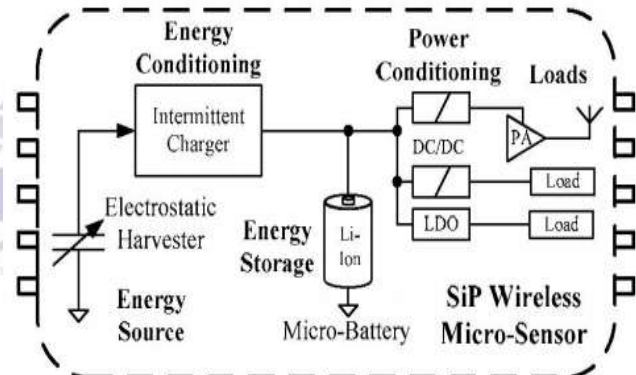


Fig. 44: Schematic of ESEH and Li-Ion Package [89]

Harvesters are used based on their size, output power, construction, form, weight, and frequency bandwidth. ESEH size depends on capacitor construction and alignment. Planner plate capacitor structures are most common, increasing harvester size. Ling Bu et al. [90] used a sidewall electric field instead of planner plate capacitor design to reduce device size. The harvester (Fig. 45) optimised for a 1 mm<sup>2</sup> array generates 0.82 μA at 20 Hz frequency and 10 μm magnitude. Testing shows the gadget can generate up to 6.45 μW of power with a load resistance of 10 MΩ.

Dongil Kim et al. proposed a liquid dielectric layer-based magnetically actuated ESEH [91]. Ferro-fluid droplets are mobile dielectrics driven by a magnetic field, resulting in capacitance fluctuation and power generation. Fig. 46

depicts a millimetre sized ESEH that generated 19.3 μW power with eight ferro-fluid droplets at 180 rpm. Numerous EHs are documented for the surveillance of human movement and various parts position and health aspects. Such devices need to have flexible substrate. One of such devices has been proposed and presented by M.E. Kiziroglou et al. [92]. A rod of 10 mm and 1.5 mm length and diameter respectively offers roughness and leads to a gap of 1 μm between rod and plate results in a capacitance of 90 pF. The device shown in Fig. 47 is tested to supply 0.5 μW power.

Energy harvesters for monitoring human motion, body temperature and breathing level have been previously developed and deployed successfully. Among human physical motions and activities, breathing is the basic

most and simple possible that led Min-Ho Seo et al. [93] to utilize water layer generated by the human respiration as a changeable area electrode. The prototype (shown in Fig. 48) was tested to successfully shown charging and

discharging by respiration. The developed prototypes were of size 1 cm<sup>2</sup> and 2.25 cm<sup>2</sup> and estimated of having 2 μW/cm<sup>2</sup> power density at 1 V.

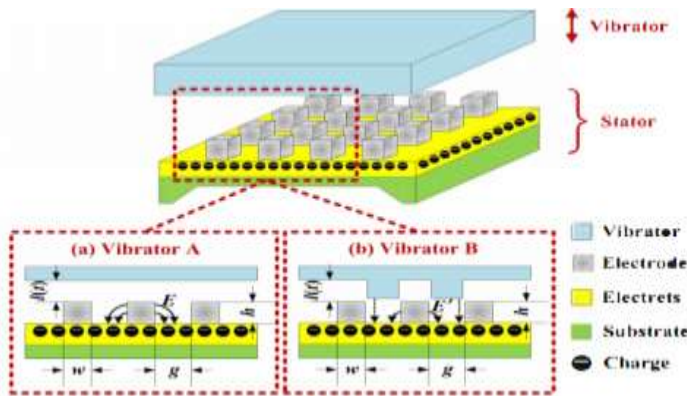


Fig. 45: ESEH array with sidewall electric field [90]

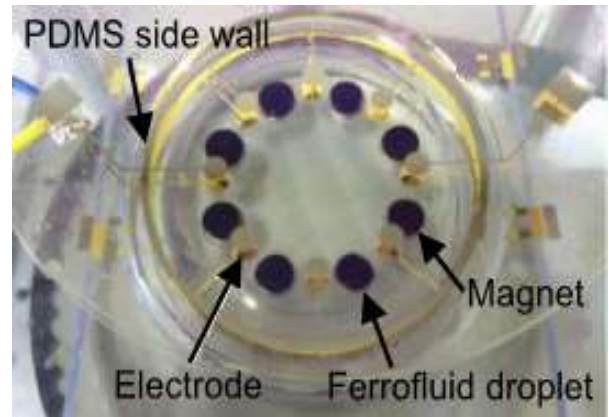


Fig. 46: Magnetically actuated ESEH [91]



Fig. 47: Flexible substrate VESEH [92]

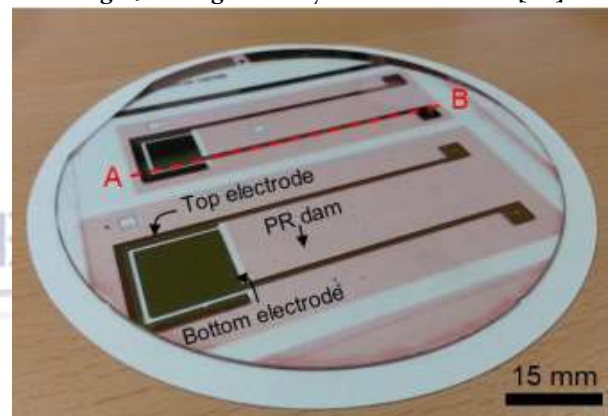


Fig. 48: VESEH based on respiration [93]

Like other EHs, electrostatic energy harvesters are important in biomedical devices. Anthony G. Fowler et al. generated ultrasonic waves using triangular electrostatic electrodes [94]. Instead of parallel finger electrodes, triangular electrostatic electrodes increase capacitance fluctuations. Electrical power was generated by mechanically stimulating a 1 mm<sup>2</sup> proof mass using electrostatic transducers using ultrasonic waves. Fig. 49 shows the harvester under a microscope. The suggested harvester generated 27.6 nW of output power from ultrasonic waves at 38.95 kHz.

T. Suzuki et al. [95] described an asymmetric multi-resonant spring-based electrostatic energy harvester employing a 13 mm x 13 mm SU-8 spring and electret structure. Fig. 50 shows a novel harvester with three vibrational modes. The spring vibrated in three modes

with various amplitudes and frequencies. In Mode 1, longitudinal vibration provided a maximum amplitude of 950 μm at 117 Hz and a maximum output power of 7.48 nW at 110 Torsional modes 2 and 3. Mode 2 generated 2.19 nW peak power-out at 165 Hz with a maximum amplitude of 532 μm at 172 Hz Mode 3 excitations had a maximum amplitude of 490 μm at 245 Hz and a maximum output of 1.72 nW at 243 Hz.

What type of vibration-based energy harvester is used depends on the operational environment. Location-specific environmental parameters including temperature, pressure, air quality, noise, moisture, and others might affect harvester performance. Of the three basic vibration-based energy harvesters, electrostatic is more temperature-resistant. Sungil Bang and Sehwan Kim confirmed this [96]. Fig. 51 shows the temperature-ESEH experiment.

Applying the proposed harvester with a 190.6 Hz vibration at  $1 \text{ m/s}^2$  amplitude and varying temperatures from  $30 \text{ }^\circ\text{C}$  to  $70 \text{ }^\circ\text{C}$  showed no significant change in power densities. It was confirmed that electrostatic energy harvesters are more temperature-resistant.

An electret-based energy harvester designed for wireless sensor applications has been reported by M. R. Ahmad and M. H. Khir [97]. The conceptual diagram of the proposed Electret Static Energy Harvester (ESEH) is

shown in Fig. 52. A 4 poles rotor along with a 4 poles stator with similar electrodes geometry were designed with  $9 \text{ }\mu\text{m}$  thick Teflon as dielectric material and placed on stator to simplify the arrangement and ease the rotor with its movement. The overlap of stator and rotor resulted in producing power. When supplied with an electret potential of  $50 \text{ V}$  and operated at a rotational speed of  $4170 \text{ rpm}$ , the device could produce an output power of  $25 \text{ }\mu\text{W}$

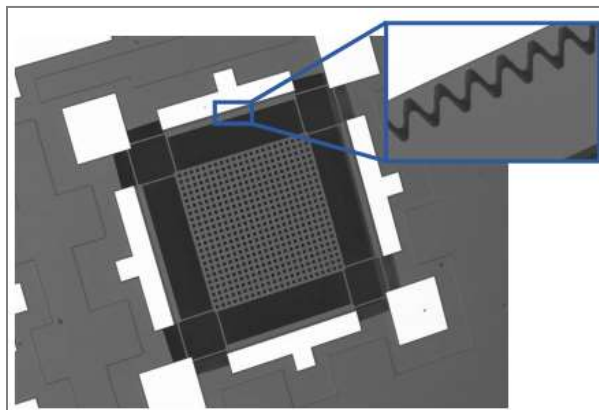


Fig. 49: SEM image of ultrasonic ESEH [94]

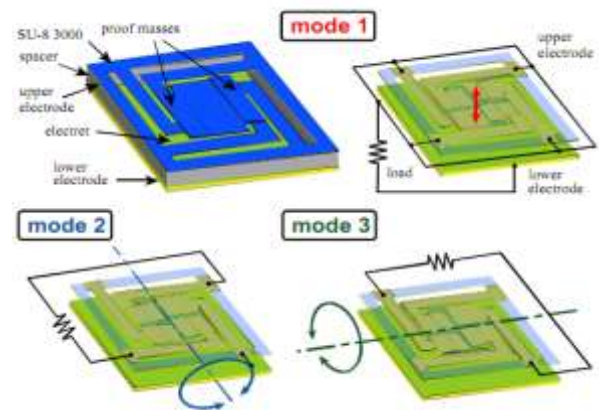


Fig. 50: ESEH along with three vibrational modes [95]

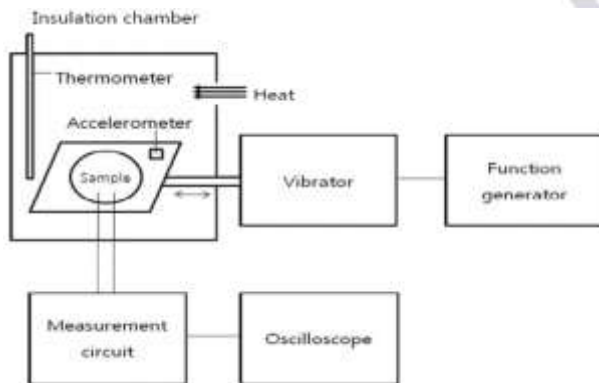


Fig. 51: The experimental set up for VESEH [96]

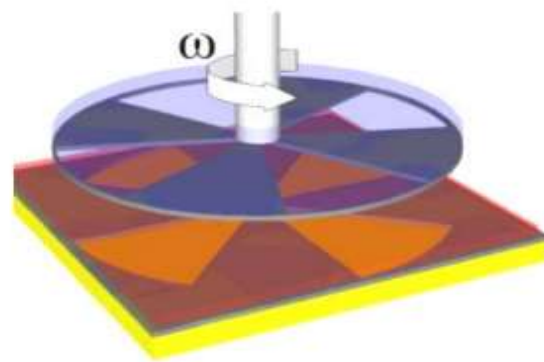


Fig. 52: Schematic diagram of ESEH [97]

R. Guillemet et al. [98] presented the trapezoidal shape gap closing based ESEH, where the capacitance electrode's design increases the transducer capacitance even after the mobile electrode contacts the stoppers, generating electrical power for remote wireless sensor nodes. Stoppers between mass and frame prevent short circuits between fixed and movable fingers and the mobile mass attached to the strong framework by four linear serpentine springs. The ESEH in Fig. 53 generated  $2.2 \text{ }\mu\text{W}$  power with  $1 \text{ g}$  external acceleration at  $150 \text{ Hz}$

frequency. High-voltage needle arrays improved charge distribution uniformity. Needles and metallic grid in conventional charging procedure discharge and charge. ESEH was evaluated to convert  $0.05 \text{ g}$  and fewer than  $100 \text{ Hz}$  excitations to reasonable output power. One out-of-plane mode at  $66 \text{ Hz}$  and two in-plane modes at  $75$  and  $78.5 \text{ Hz}$  were used.

According to Abdulmunam et al. [99], the simulink model (Fig. 54) of an integrated rotating ESEH is ideal for wind-energy scavenging and remote wind speed

monitoring. The device has a small wind turbine rotor blade that intake wind, a rotating variable capacitor in the electrostatic converter, storage, and load. Simulation results showed that a variable rotor capacitor of 50 pF–550 pF subjected to 15 mph wind velocity harvested 0.87 mA average current and 2.46 mW power in 147 ms. Based on recent design, P. Pondrom et al. suggested compact electret VESEHs [100]. The proposed harvesters

(Fig. 55 schematic diagram) used electret surface potential between 400 V and 10 gm seismic mass to eliminate the need for a battery for start-up voltage. This compact electret harvester could harvest 0.6 mW peak power at 36 Hz and 1 g acceleration, making it ideal for low-frequency environmental excitations.

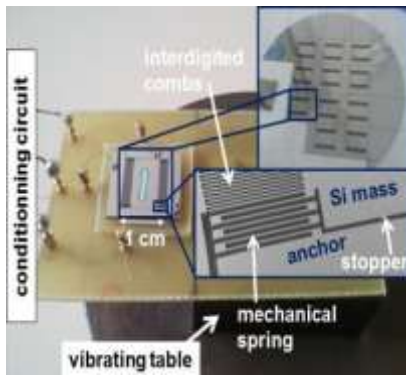


Fig. 53: Fabricated ESEH [98]

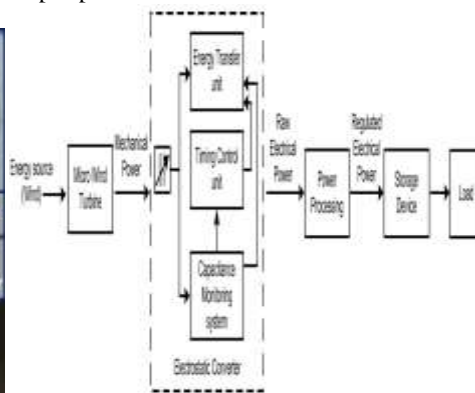


Fig. 54: Block diagram of ESEH [99]

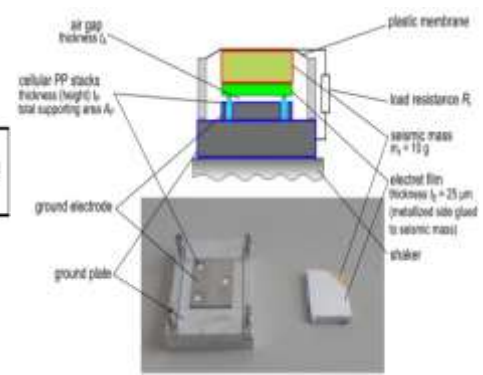


Fig. 55: The compact ESEH [100]

IV. (B) NON-RESONANT VESEHs

A non-resonant VESEH uses relative motion of electrodes to generate electrostatic forces extracting energy from vibrations. Unlike resonant harvesters, these devices depend not on specific resonance frequencies but rather operate efficiently throughout a wider frequency band.

Many applications require powering autonomous wireless sensor nodes at various frequencies. A low-frequency ESEH by Y. Lu et al. [101] is a wide-band harvester for remote temperature wireless sensor nodes. Using a 2 g vibration level, this device collected over 1 μW power over 59-148 Hz frequency range. Fig.56 shows the gadget and schematic.

Khaled Ramadan et al. [102] presented an ESEH to gather environmental vibration energy. The gadget, measuring 0.35 mm<sup>3</sup> (1.5 mm × 1.5 mm × 0.15 mm), was made of SU-8 material for the spring and proof mass. Three device models were evaluated at 50, 75, and 110 Hz. The construction (Fig. 57) demonstrated a power

density of 0.032 μW/mm<sup>3</sup> under 10 μm external vibrations at 110 Hz with a 6 V input voltage.

A typical electrostatic energy harvester has one fixed and one moving plate to vary capacitance with vibration. Ai Zhang et al. [103] developed a broad bandwidth ESEH with virtually equal resonant frequencies using two cantilever-mass structures as electrodes in a parallel-plate configuration. Due to coupling effect, the two cantilever system's overall frequency was greater than each cantilever's resonant frequency. The gadget is depicted in Fig. 58. With an external vibration of 4.5 m/s<sup>2</sup> at 42-50 Hz, the peak power-out ranged from 22 to 35 μW with a load resistor of 300 MΩ.

Ling Bu et al. proposed a vertical gap shifting, non-resonance wideband ESEH [104]. Fig. 59 shows the vertical gap altering procedure and wide-band ESEH. A peak output of 0.2 μW to 0.7 μW was achieved at frequencies between 5 Hz and 120 Hz with a 2 mm gap between the electrodes.

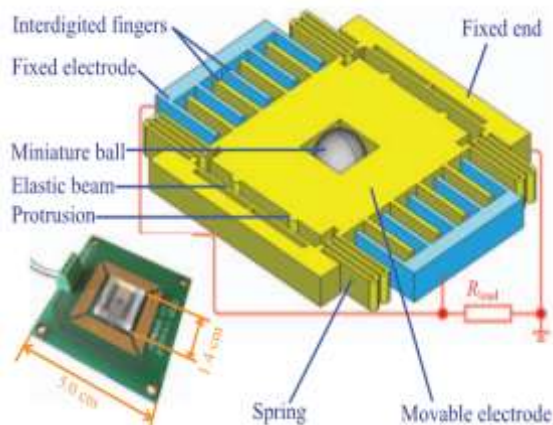


Fig. 56: Fabricated EH and its schematic diagram [101]

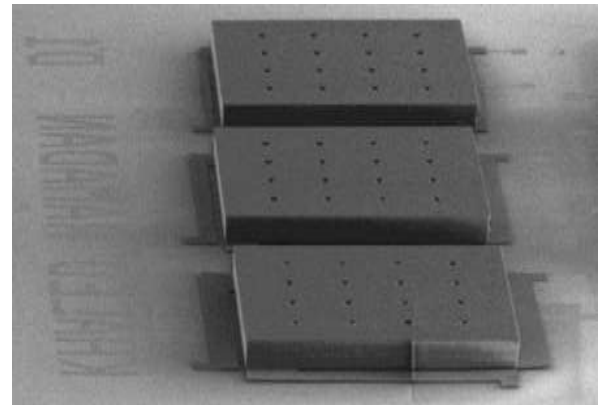


Fig. 57: Fabricated ESEH[102]



Fig. 58: Proposed broad bandwidth ESEH[103]

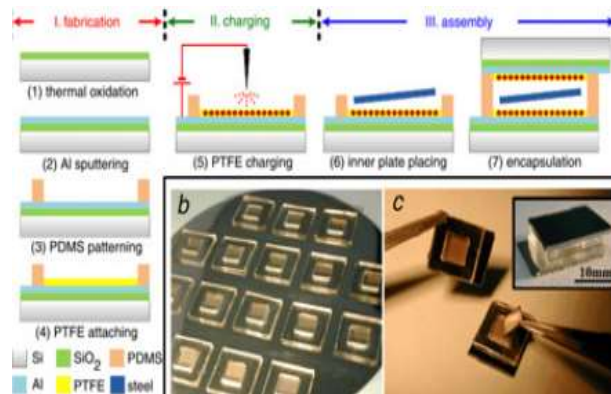


Fig. 59: Vertical gap closing Non-resonant EH [104]

Son Duy Nguyen et al. [105] proposed using non-linear springs in electrostatic energy harvesters and found that for 50 Hz random vibrations with varying central frequency, the output was lower than for linear springs, but for 38 Hz and 58 Hz below the central frequencies, the output was higher. The EH with non-linear spring (Fig. 60) was tested for output power. The non linear spring harvester produced  $7 \mu\text{W}$  of output power at 120 V bias voltage and 0.36 g acceleration.

A low acceleration and low frequency vibrations excited ESEH was proposed and built by K. Tao et al. [106]. High-voltage needle arrays improved charge distribution uniformity. Needles and metallic grid in conventional charging procedure discharge and charge. Fig. 61 illustrates the electret-based VESEH schematic. The electrostatic energy harvester converted 0.05 g and fewer than 100 Hz excitations to useable output power. The gadget had one out-of-plane and two in-plane modes at 66Hz, 75Hz, and 78.5Hz.

VESEHs with low frequency and acceleration have been proposed by M Pourahmadi Nakhli et al. [107] to gather cardiac energy for pacemakers. The 3D VESEH combined in-plane overlap and gap closing to efficiently absorbing heartbeat-released energy. Compound 3D ESEH capacitor structure is depicted in Fig. 62. The 3D feature boosted power output to  $35.038 \mu\text{W}$  at the same size, surpassing the new rates of in-plane overlap and gap-closing electrostatic harvesters. The 3D VESEH is suitable for low frequencies of 1-100 Hz and accelerations of 0.05 to 0.6 g. The designed harvester, measuring  $5000 \times 5000 \times 100 \mu\text{m}^3$  ( $0.0025 \text{ cm}^3$ ), produces  $49.04 \mu\text{W}$  at 31 Hz and 0.6 g acceleration.

Yulong Zhang et al. demonstrated a wide-band VESEH [108]. The developed EH in Fig.63 had two sections. The bottom stationary plate and top adjustable plate were made from silicone wafer using traditional MEMS processes. The harvester conceptual drawing is shown in Fig. 63. The variable capacitor's starting gap was controlled by the upper plate, which had a proof mass

hanging from an external frame via a four-spring structure, and the bottom plate, which had a cavity. The bottom electrode was an electret due to CYTOP polymer covering. Proof mass had stoppers to prevent electrostatic force from pulling it towards the base electrode during

excessive vibration. The VESEH device had a volume of  $0.187 \text{ cm}^3$  and generated  $4.95 \text{ }\mu\text{W}$  power at  $0.9 \text{ g}$ ,  $136 \text{ Hz}$ , and  $12 \text{ Hz}$  bandwidth, resulting in  $26.47 \text{ }\mu\text{W}/\text{cm}^3$  power density.

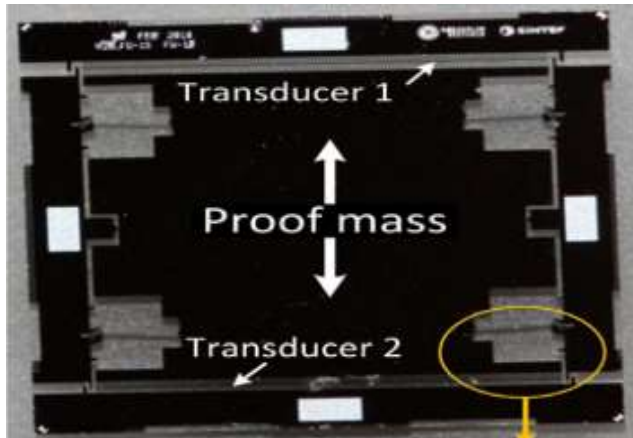


Fig. 60: Proposed non linear springs based ESEH[105]

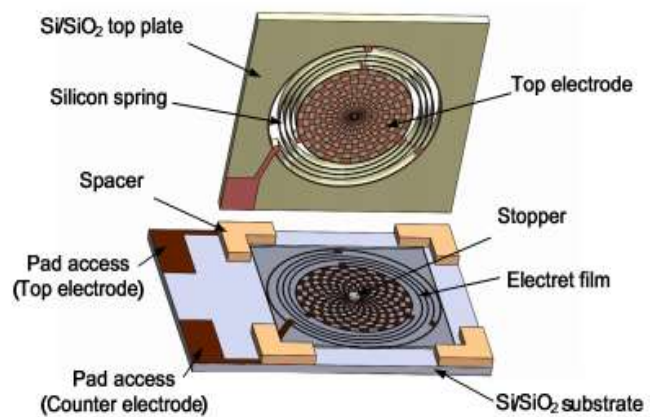


Fig. 61: ESEH's schematic based on electrets [106]

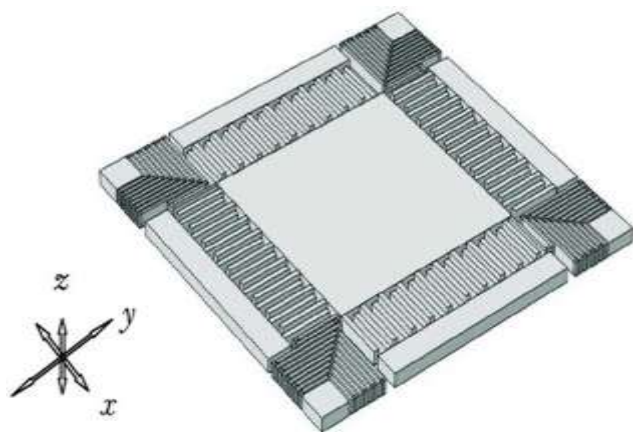


Fig. 62: Capacitor's structure of 3D ESEH [107]

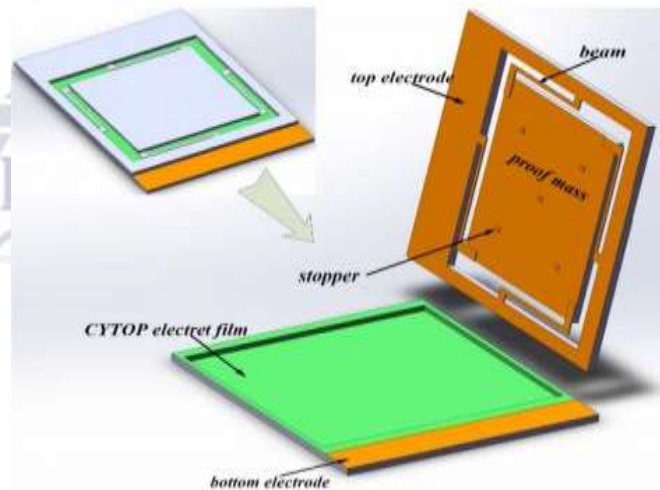


Fig. 63: 3D schematic of the developed ESEH [108]

Yamane et al. designed an EDLE-based contactless vibration electrostatic energy harvester [109]. Unlike contact-type VESEHs, the moveable electrode and electret always have an air gap. Fixed charges on the surface double layer electrets created charges on the moveable electrode. Incident vibrations changed the overlapping region between double layer electrets and movable electrode, causing induced charges to change and electric current to flow through an external load. EDLE expanded the working frequency range and made the device usable for resonant and non-resonant circumstances. Four  $12.5 \text{ mm}^3$  EDLEs were used to create an energy harvester that

generated  $4 \text{ pA}$  RMS output current at  $1 \text{ g}$  and  $159 \text{ Hz}$  stimulation. Normalised power density was  $2 \times 10^{-7} \text{ W}/\text{cm}^3/\text{g}^2/\Omega$ . The frequency vs output current graph showed a 20-Hz bandwidth ( $145\text{--}165 \text{ Hz}$ ). Fig. 64 shows the developed VESEH.

Vysotskyi et al. [110] presented VESEH autonomous dual-side capacitive transducer architecture (Fig. 65) for biomedical applications with increased bandwidth. Basic silicon-on-glass technology was used to build the proposed VESEH on a PCB. The moveable section's tungsten auxiliary mass lowered the resonance frequency, making it suited for low-frequency appliances. At  $30 \text{ V}$  bias voltage

and 40.8 Hz vibration intensity, frequency bandwidth increased by 280%. Device dimensions were 22 mm x 5.6 mm.

H. Honma et al. [111] constructed a non-resonant VESEH with high density electret film short stroke comb electrodes. This high-density electret film improved power conversion in comb electrodes. Tungsten blocks weighing 2.2 gm were placed on moveable electrodes to boost energy output. The energy harvester measured 1 cm x 1.5 cm x 0.38 cm (volume = 0.57 cm<sup>3</sup>) and featured 1573 combs of 50 μm length and 10 μm width. The frequency bandwidth increased 3.6 times from 18 Hz to 64 Hz when the electret potential was adjusted from -200 V to -300 V. The planned VESEH had a normalised power density of

700 μW/cm<sup>3</sup>/g<sup>2</sup>. Fig. 66 shows the energy harvester and SEM view.

M. Li et al. [112] designed a wafer-scale self-rechargeable electret-based VESEH. With embedded silicon tips, the electret could be recharged inside the device container without detaching. Holes on fixed electrodes minimised air damping and improved output voltage. The harvester produced 6.2 V at 75 Hz when self-charged. The described harvester had a bandwidth of 10 Hz at 0.5 g acceleration and 27 Hz at 1 g excitation. The device's output power was 0.37 μW at 64 Hz and 1 g acceleration, with a power density of 1.58 μW/cm<sup>3</sup> and a volume of 0.234 cm<sup>3</sup>. Fig. 67 shows the developed harvester diagrammatically.

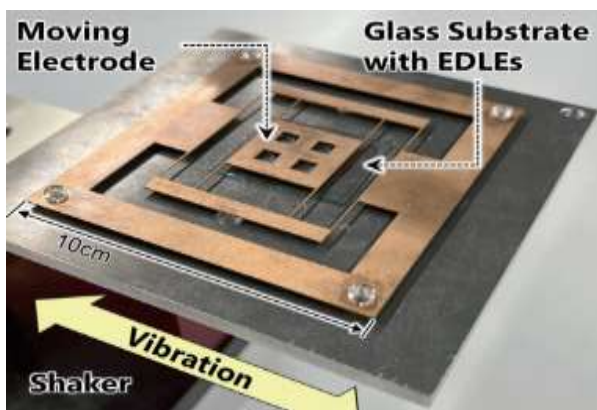


Fig. 64: Developed contactless EDLE VESEH [109]

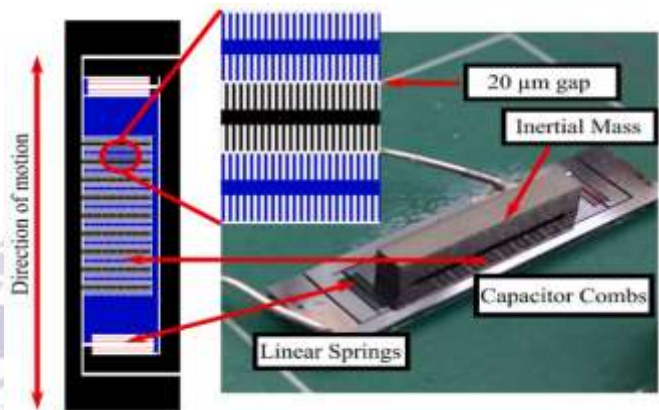


Fig. 65: Picture and schematic of the VESEH [110]

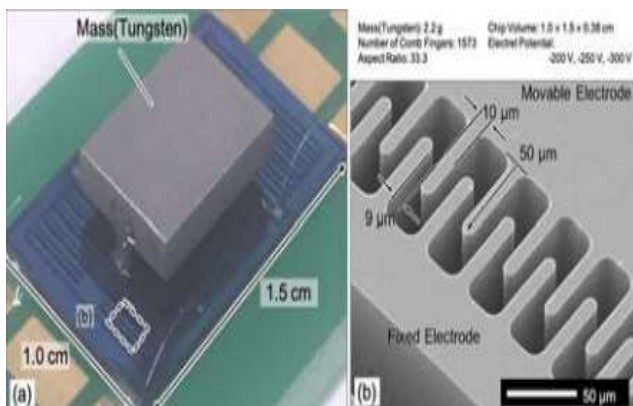


Fig. 66: (a) VESEH and (b) Comb electrodes [111]

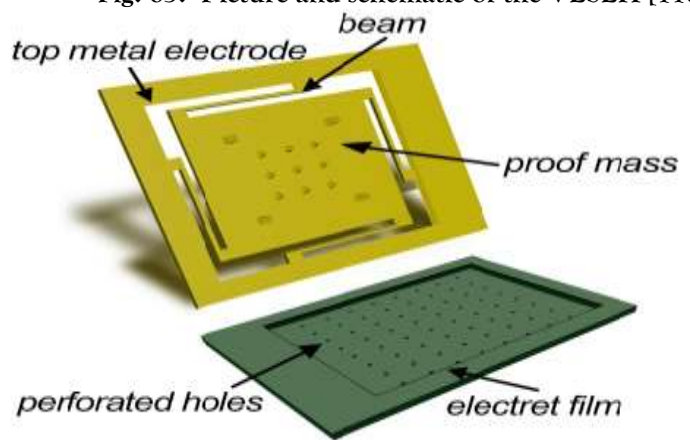


Fig. 67: Schematic of the proposed VESEH [112]

#### IV. (C) COMPARISON OF THE REPORTED VESEHS

This evaluation compares VESEHs based on their volume, vibration acceleration, operating frequency range, voltage output, power output, and power density.

Table IV compares harvesters depending on their parameters.

Fig. 68 compares resonant and non-resonant harvesters by size and average power production. In Fig. 68, Min-Ho Seo et al. [93] reported the largest harvester, a resonant

device with 2.25 cm<sup>3</sup> total volume and 4.5 μW output power, resulting in 2 μW/cm<sup>3</sup> power density. The non-resonant device in [107] is the smallest (0.0025 cm<sup>3</sup>) and generates 49.04 μW of power with a power density of 19616 μW/cm<sup>3</sup> among documented VESEHs. The relationship between power density and acceleration for the reported VESEHs is depicted in Fig. 69. The

device described in [107], a non-resonant harvester, achieves a maximum power density of 19616 μW/cm<sup>3</sup>, but the resonant device detailed in [96] has a minimum power density of 0.52 μW/cm<sup>3</sup>. Overall, the power density of the non-resonant type VESEHs is higher than that of resonant type VESEHs.

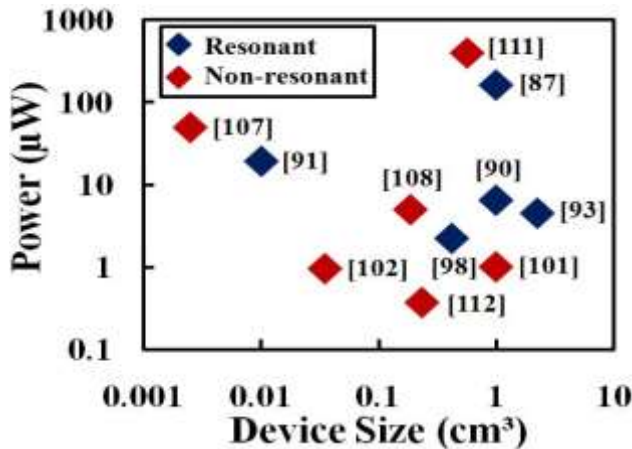


Fig. 68: Power generated vs. device volume of VESEHs

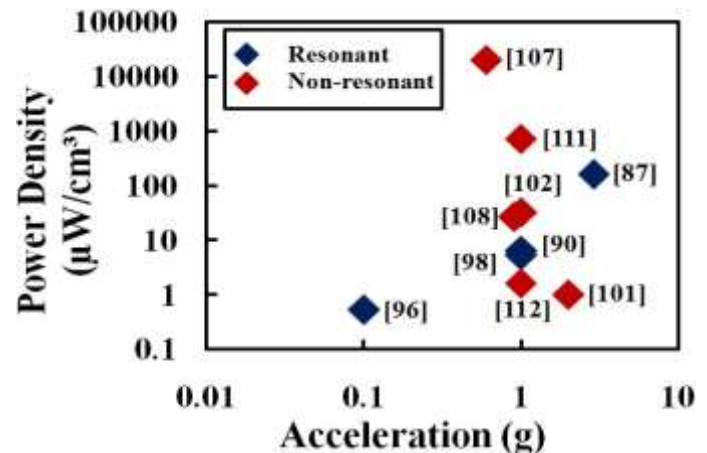


Fig. 69: Power density vs. acceleration of VESEH

Power per acceleration as a function of device size is shown in Fig. 70. The highest value of power per acceleration is 399 μW/g which is offered by the harvester reported in [111] which is a non-resonant device. The lowest value of power per acceleration is 0.37 μW/g which is reported for the harvester in [112]. Fig. 70 also clearly shows that resonant VESEHs are generally larger in size, while non-resonant VESEHs deliver higher power output relative to acceleration.

Energy harvesting devices' frequency bandwidth and output power are compared in Fig. 71. According to reference [105], the broad band VESEH operates at 50 Hz but produces less than 7 μW of power. While the resonant device in [92] has a minimum frequency bandwidth of 5 Hz, its maximum output power is just 0.5 μW. Power versus frequency bandwidth shows that non-resonant VESEHs have a wider frequency bandwidth than resonant.

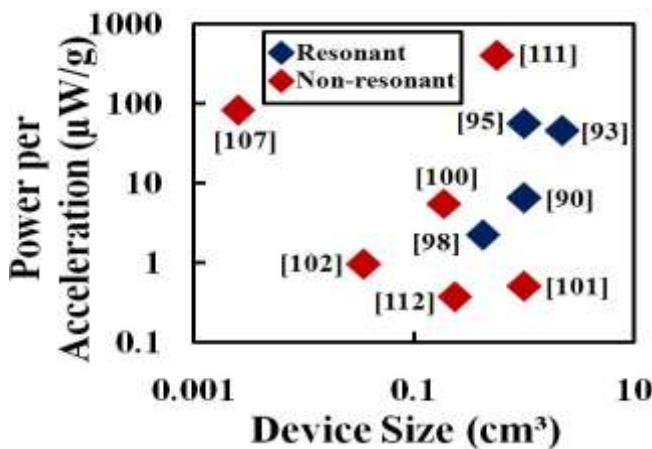


Fig. 70: Power per acceleration vs. size of VESEHs

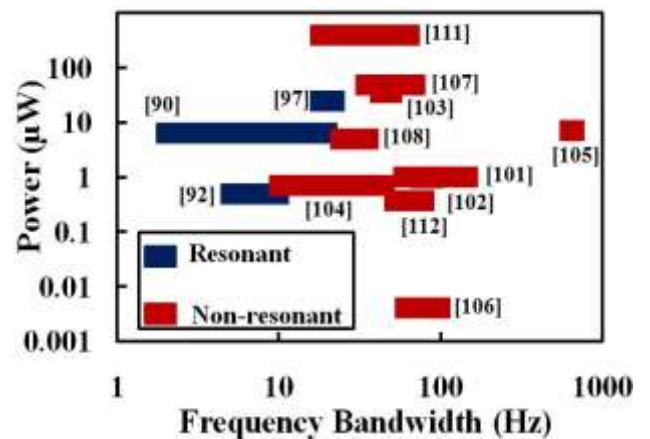


Fig. 71: Frequency bandwidth vs. power of VESEHs

Table IV: Comparative analysis of the reported VESEHs

Type	Device Volume (cm <sup>3</sup> )	Acceleration (g)	Operating Frequency Range (Hz)	Frequency Bandwidth (Hz)	Voltage (mV)	Average Power Output (μW)	Power Density (μW/cm <sup>3</sup> )	Power / Acceleration (μW/g)	Power Density/ Acceleration (μW/g cm <sup>3</sup> )	Ref.
Resonant	0.01125	-	10000 - 12000	20	-	pW	-	-	-	[86]
	1	2.9	728	-	4000	160	160	55.17	55.17	[87]
	-	-	>100	-	2400	-	-	-	-	[88]
	-	-	-	-	-	-	38	-	-	[89]
	1	1	20	-	-	6.45	6.45	6.45	6.45	[90]
	mm	-	13.3	-	-	19.3	-	-	-	[91]
	-	-	10	-	3	0.5	-	-	-	[92]
	2.25	-	10	-	-	4.5	2	-	-	[93]
	-	-	38950	-	-	0.00276	-	-	-	[94]
	-	Gap. 490um	243	-	-	0.00172	-	-	-	[95]
	-	0.1	190.6	-	-	-	0.52	-	5.2	[96]
	-	1	20	-	-	25	-	-	-	[97]
	0.42	1	150	-	-	2.2	5.24	2.2	5.24	[98]
	-	15Mph wind speed	147m sec period	-	0.87mA	246	-	-	-	[99]
-	1	36	-	-	600	-	-	-	[100]	
Non-resonant	1	2	59-148	-	-	1	1	0.5	0.5	[101]
	0.035	1	75-110	15	-	0.95	32	0.95	32	[102]
	-	0.45	42-50	-	-	35	-	77.77	-	[103]
	-	1mm	5-120	35	3-7	0.7	-	-	-	[104]
	-	0.36	625-675	50	-	7	-	19.44	-	[105]
	-	0.05	60-100	-	330	0.00408	-	0.082	-	[106]
	0.0025	0.6	1-100	36	-	49.04	19616	81.76	32693	[107]
	0.187	0.9	1-36	12	-	4.95	26.47	5.5	29.41	[108]
	1.25	1	145-165	-	-	-	-	-	2x10 <sup>-7</sup>	[109]
	-	-	40.8	-	-	-	-	-	-	[110]
	0.57	1	18-64	-	-	399	700	399	700	[111]
	0.234	1	52-79	27	6.2	0.37	1.58	0.37	1.58	[112]

V. VIBRATION PIEZOELECTRIC ENERGY HARVESTERS (VPEEHs)

Piezoelectric materials generate charges under stress/strain. High frequency and acceleration are needed to strain the material in these devices. The capacity of piezoelectric-based MEMS to gather modest amounts of

energy from environmental vibrations is well recognised. This breakthrough has enabled modern wireless sensor nodes to operate without batteries or cumbersome wiring, bringing us closer to battery-free sensor systems and networks [113]. A cantilever-based piezoelectric EH harvests energy from environmental vibrations at each

cycle through base excitation. Mechanical strain is stored in the beam as potential energy after being converted to proof mass kinetic energy. Induced charges across the beam's piezoelectric layer convert some of its flexible energy into electrical energy [113]. Lead zirconate titanate (PZT) is used in bimorph or unimorph cantilever beam piezoelectric energy harvesters.

The cantilever beam's resonance frequency can be matched to environmental vibration frequency by attaching a proof mass. Many VPEEHs have been designed and built to power remote wireless sensor nodes. The following section compares the size, resonance frequency, output power, and power densities of several produced harvesters.

#### V. (A) RESONANT VPEEHs

A resonant VPEEH generates energy from mechanical vibrations at the material's inherent frequency. Aligning vibrations with resonance frequency and employing piezoelectric materials that generate an electric charge under mechanical pressure improves vibrations. When the harvester experiences vibrations around its resonance frequency, their amplitude increases, increasing mechanical stress on the piezoelectric material. Increased mechanical stress on piezoelectric material boosts electric charge production and voltage output.

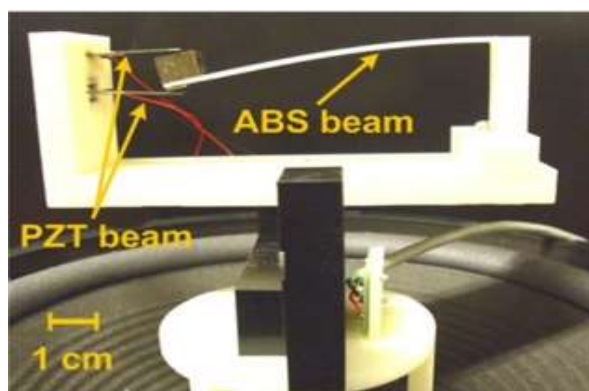


Fig. 72: Fabricated low frequency VPEEH [114] [115]

Jing Qiu et al. [116] proposed powering wireless sensor nodes that monitor electric lines with a piezoelectric energy harvester. Fig. 74 depicts the proposed harvester, which includes a cantilever beam, a NdFeB permanent magnet, a magneto-electric (ME) transducer, and

A low-frequency ambient vibrations-based piezoelectric energy harvesting system by Lei Gu [114] has a single proven mass-carrying driving beam and two firm power-producing beams. The driving beam was an 8-gm mass-bearing acrylonitrile butadiene styrene (ABS) beam, while two stiff PZT bimorph beams, each 2.6 cm x 0.64 cm x 0.051 cm, generated electricity. The periodic contact between the driving and generating beams turned low-frequency ambient vibrations into high-frequency resonance. This configuration reduced driving beam movement and increased power density. The low frequency piezoelectric EH in Fig.72 generated 1.53 mW average power at 20.1 Hz and 0.4 g acceleration, leading in 93.2 mW/cm<sup>3</sup> power density.

Unlike ambient vibrations, resonance-based EHs have high frequency and low output power limits. This requires up-converting the ambient frequency or reducing the harvester's resonance frequency. Lokesh Dhakar et al. [115] propose a composite cantilever piezoelectric EH with proof mass at the beam's free tip. As shown in Fig. 73, the composite cantilever energy harvester uses a longitudinally coupled bimorph piezoelectric and polymer beam. This composite cantilever beam lowered the EH's resonance frequency to 36 Hz. During testing at 0.2 g acceleration, the device produced a maximum output power of 40  $\mu$ W with an output voltage of 3.3 V. The bandwidth reached 16.4 Hz with 2.5 g acceleration.

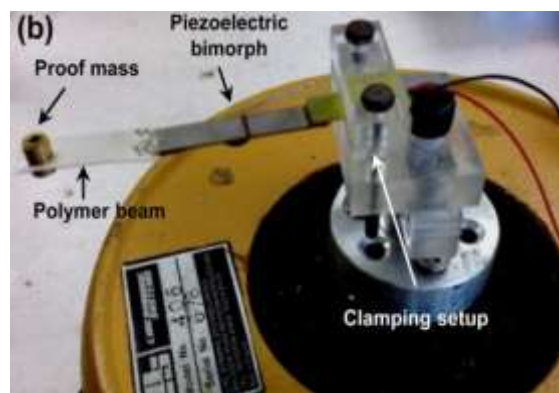


Fig. 73: The Constructed composite cantilever VPEEH

magnetic yokes as proof masses. The 10 mm x 24 mm x 0.8 mm PZT transducer is in the EH cover. The beryllium bronze cantilever beam was 60 mm x 20 mm x 0.5 mm and secured to an aluminium holder at both ends. The ME transducer detected the magnetic field from the

electric lines around the work area. Test results show the device producing 56.1 V output voltage and 240  $\mu\text{W}$  average power at 3A line current and 50 Hz frequency. The peak output power of 503  $\mu\text{W}$  at 50 Hz was reached with an 8 A current.

Y. Wang et al. [117] built an air-driven closed chamber sealed PEEH with a 25 mm diameter PZT piezoelectric flexible patch that transformed hyperbaric air energy into



Fig. 74: Proposed VPEEH for electric lines [116]

Gang Tang et al. created a  $d_{33}$  mode single crystal piezoelectric using PMN-PT and silicon [118]. A  $2900 \mu\text{m} \times 800 \mu\text{m} \times 25 \mu\text{m}$  cantilever with  $10 \mu\text{m}$  PMN-PT piezoelectric layer,  $13 \mu\text{m}$  supporting silicon layer, and  $900 \mu\text{m} \times 800 \mu\text{m} \times 500 \mu\text{m}$  nickel proof mass comprised the device. PMN-PT piezoelectric thick film improved coupling and electromechanical coefficients. Interdigitated electrodes improved  $d_{33}$  mode EH conversion efficiency. The PMN-PT thick film was created using wafer bonding and mechanical lapping. The harvester prototype (Fig. 76) with  $0.418 \text{ mm}^3$  effective volume was tested at 1.5 g excitation level and resonance frequency of 406 Hz, achieving 5.3 V peak output voltage, 7.182  $\mu\text{W}$  power, and 17.18  $\mu\text{W}/\text{mm}^3$  power density.

Most piezoelectric energy harvesters use  $d_{31}$  mode, although some, like [106], use  $d_{33}$  mode. H. J. Jung et al. presented an impact-based hybrid PEEH using both modes [119]. The harvester used  $240 \text{ mm} \times 35 \text{ mm} \times 45 \text{ mm}$

electrical energy through piezoelectric deformation. Fig. 75 shows a harvester with a closed chamber, air inlet, PZT patch, and copper substrate. The incident air caused the PZT patch to distort, generating electrical energy due to the pressure differential between the closed chamber and closed micro chamber. At 365 l/min air flow, 0.4 MPa pressure, and 0.8 sec cycle duration, the device produced 3.41 mW of effective power over a 200 k $\Omega$  load resistor.

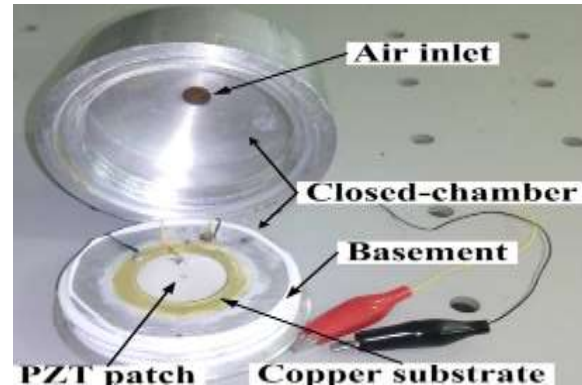


Fig. 75: Constructed closed chamber VPEEH [117]

0.2 mm piezoelectric modules and a multi array rectifying circuit to rectify each module's output and combine it in parallel. Rotation was communicated to the harvester by a 4:1 chain and gear, increasing impact frequency. The hybrid PEEH in Fig. 77 generated 20 V and 215 mA current at 13 rpm from a wheel, producing 4.3 W of output power at 20 Hz impact frequency across a 100  $\Omega$  load.

Y. H. Seo et al. [120] developed a wind flow-based PEEH for building and bridge health monitoring. The harvester prototype consisted of four slightly bent piezoelectric film-covered silicon cantilevers measuring  $2,000 \mu\text{m} \times 200 \mu\text{m} \times 3.5 \mu\text{m}$ . When exposed to wind, piezoelectric-based bent micro-cantilevers generated electricity from flow-induced ambient vibrations. The device in Fig. 78 was tested at 12.4 m/s wind speed, generating 1.77  $\mu\text{W}$  of output power at 1.88 V and 441.8  $\mu\text{W}/\text{cm}^3$  of power density.

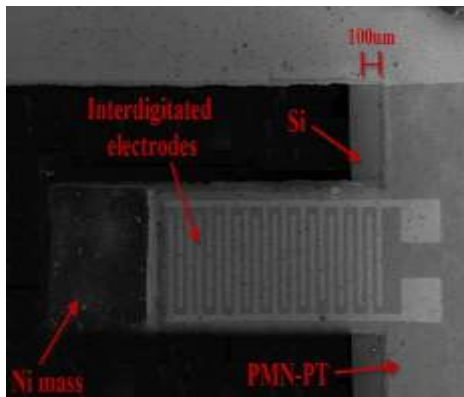


Fig. 76: Proposed PMN-PT EH [118]

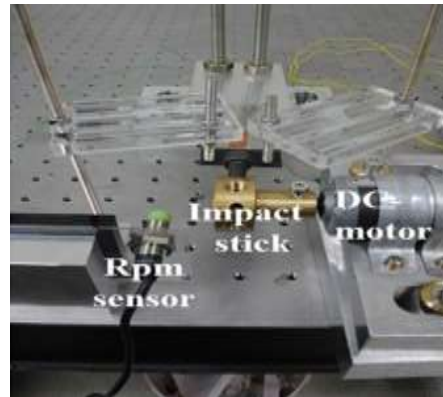


Fig. 77: Experimental VPEEH [119]

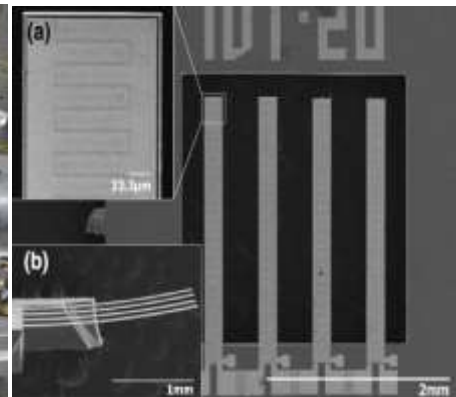


Fig. 78: Schematic of VPEEH [120]

P. K. Panda et al. [121] proposed comparing two sets of PZT-based PEEHs in multilayer stacks and bimorph architectures. Both stacks and bimorph structures were tape cast. The 110  $\mu\text{m}$  thick 100 layers were used to create multilayered stacks with an active volume of 8 mm x 6 mm x 10 mm. Bimorph structures were created utilising the same tape casting procedure. Multilayer stacks and bimorph structures are shown in Fig. 79(a) and 79(b). The multilayer stacks and bimorph output was sent to the output load resistor via a bridge rectifier and capacitor and compared for vibrations. Each structure was measured at 24 Hz after a 10-minute cycle. The output voltage of multilayer stacks was 125 mV and bimorph structure 450 mV.

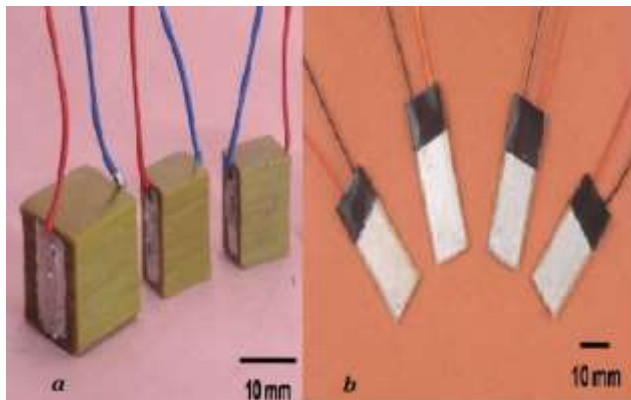


Fig. 79: (a) Multilayer stacks (b) bimorph [121]

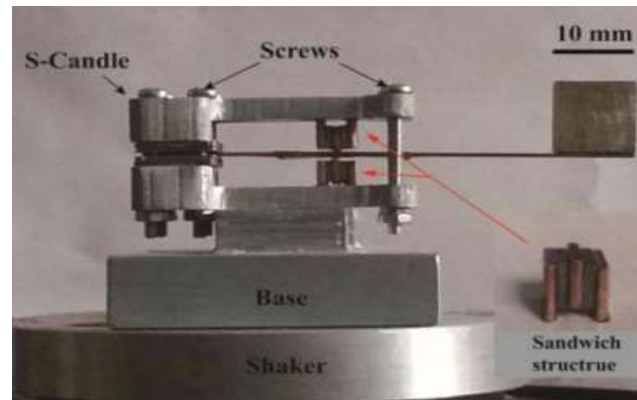


Fig. 80: Constructed cantilever based EH [122]

Z. Zeng et al. developed a sandwich-structured cantilever-driven PMN-PT single crystal harvester using shear mode low-frequency vibrations [122]. Three 3.6 mm x 6 mm x 1 mm copper blocks sandwiched two PMN-PT wafers electrically coupled in series to make the device. This candle-shaped energy harvester was developed using an aluminium alloy frame holding this sandwich construction and a 55 mm x 6 mm 0.6 mm cantilever with proof mass at the tip. The cantilever conveyed base excitation vibrations, which pressed the sandwich structure and frame, deforming the wafers between the copper blocks and creating electrical charges. The prototype (Fig. 80) demonstrated 60.8 V open circuit voltage and 10.8  $\text{mW}/\text{cm}^3$  power density with 13.5 gm proof mass, 1 g acceleration, and 43.8 Hz frequency.

### V. (B) NON-RESONANT VPEEHs

A non-resonant VPEEH turns mechanical vibrations into electricity regardless of its fundamental frequency. The piezoelectric action instantly converts mechanical strain into electrical charge. This strain can be caused by

collision, friction, or magnetic interaction. Resonant harvesters are tuned for certain frequencies, whereas non-resonant harvesters work efficiently with several mechanical inputs and a wider frequency range. This allows them to use diverse environmental energy sources.

A. Alomari and A. Batra [123] created a series of unimorph piezoelectric cantilever beams with uniform thickness and width but different lengths to increase bandwidth and power. Five PVDF unimorph cantilever beams were attached to the aluminium beam's front. The device had five modes with varied frequencies and output powers. The harvester in Fig. 81, measuring 100 mm x 65 mm x 0.5 mm, was tested with a broad bandwidth of 22 Hz to 88 Hz and output voltage of 0.17 V to 0.72 V from 0.29  $\mu$ W to 5.22  $\mu$ W.

M. Guan and Wei-Hsin Liao [124] developed a rotating motion-based PEEH for powering wireless sensor nodes, especially for tyre pressure monitoring systems. The harvester in question transformed mechanical energy into electrical energy by repeatedly deforming piezoelectric materials while moving. On either side of the beam were

two PZT 50 mm x 50 mm x 1.734 mm piezoelectric components. The device shown in Fig. 82 was tested from 7 Hz to 13.5 Hz, resulting in an average output power of 83.5  $\mu$ W to 825  $\mu$ W.

Z. Chew and L. Li built a piezoelectric wide-frequency harvester [125]. The harvester used 9 piezoelectric bimorph constructions each 15 mm x 1.4 mm x 0.6 mm, linked so that the first beam was fastened on a PCB board and the other suspended end was coupled to a second identical beam joined together with epoxy glue. Other identical beams were linked with the 9th on top and free end. Seven resonant peaks were found in this 9-beam design from 100 to 1000 Hz. A 130 Hz external vibration produced a maximum output voltage of 3.58 V and a power of 20.5  $\mu$ W over a 10 k $\Omega$  resistor. Fig. 83 shows PEEH fabrication.

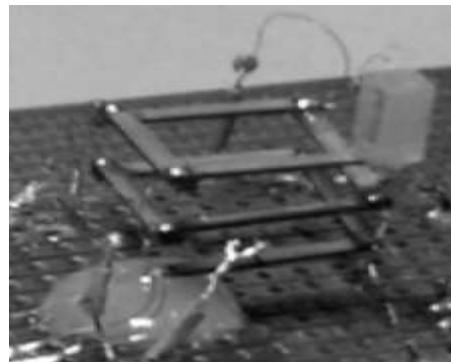
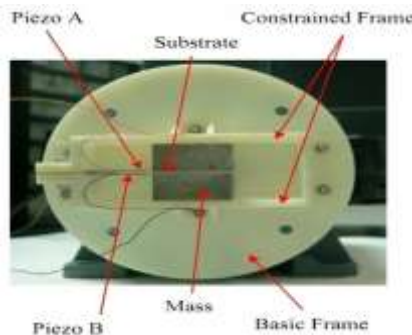


Fig. 81: Multi-cantilever beams array [123] Fig. 82: Fabricated VPEEH [124] Fig. 83: Fabricated VPEEH [125]

D. Vasic et al. [126] built a simple PEEH for low-frequency and low-amplitude ambient vibration and tested it on four cycling sites. The harvester was made of PZT piezoelectric material and divided into three segments: the largest patch,  $P_1$ , measuring 3.8 cm x 1.6 cm x 0.03 cm, provided main energy, the second smaller patch,  $P_2$ , powered the driving electronics, and the third smaller patch,  $P_3$ , measured velocity and generated driving signals. Three patches were stacked on a steel beam of 8.3 cm x 2.6 cm x 0.025 cm, with a mass of 5.32 gm at the tip, adjusting the working frequency from 14 Hz to 25 Hz. The overall device size was 2.37 cm<sup>3</sup>. A power of 3.4 mW was achieved at 18.8 Hz and 21 km/hr with a load of 200 k $\Omega$ . Fig. 84 shows the harvester.

Taemin Kim et al. [127] proposed a wide-band PEEH with four piezoelectric layers on a substrate, each with a different resonance frequency. The harvester, depicted in Fig. 85, is 3.9 cm<sup>3</sup> and measures 61 mm x 160 mm x 0.4

mm in length, width, and thickness. At 120 Hz and 1.5 g acceleration, the PEEH produced 321 mW peak power. The operational frequency bandwidth was 6 Hz (117–123 Hz).

Shim et al. [128] presented a linked beam array nonlinear wide-band VPEEH. By integrating the coupled beam array's structural non-linearity and multi resonance in coupling effect, the proposed harvester increased the operational frequency bandwidth. Four distinct frequency piezoelectric beams, two elastic supports, and a base composed the VPEEH (Fig. 86). The coupling impact of elastic supports caused non-linearity, increased output voltage, and broadened operational frequency bandwidth. At 1 g acceleration, the energy harvester produced 144.2% more power than four identical freestanding beams from 40 to 80 Hz. The new energy harvester had 93.3% more frequency bandwidth. Each beam measured 14 cm x 1 cm x 0.05 cm, and the connected beam array

harvester had an estimated 28 cm<sup>3</sup> volume. Optimal harvester power output was 92.2 mW at 1 g and 57 Hz.



Fig. 84: Fabricated VPEEH [126]



Fig. 85: Fabricated VPEEH [127]

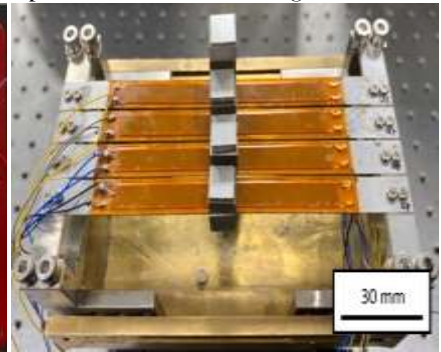


Fig. 86: Coupled beam VPEEH [128]

Fan et al. [129] constructed and tested a non-linear wide-band VPEEH under direct and parametric stimulated circumstances. The gadget has four piezoelectric layers and four cantilever beams with different tip masses. Two pairs of limiters restricted beam mobility. Motion limiters caused non-linearity and frequency hardening, increasing frequency bandwidth from 5.7 Hz to 12.3 Hz. Four beams were measured as follows: A: 17 cm x 1.15 cm x 0.05 cm, B: 17.9 cm x 1.18 cm x 0.05 cm, C: 17.4 cm x 1.15 cm x 0.05 cm, and D: 18.1 cm x 1.08 cm x 0.05 cm, with an estimated volume of 4 cm<sup>3</sup>. These beams have tip masses of 0.972, 0.964, 1.931, and 3.169 gm. At 0.2 g and 6.2 Hz, the harvester produced 1.7 V and 6.5 mW. Fig. 87 shows the built apparatus.

Zhang et al. [130] developed a layered piezoceramic VPEEH to generate energy from non-harmonic vibrations. Stacked piezo-ceramics were made by multilayer adhesion. The piezoceramic sheets were multilayered and alternated with flexible electrodes. Copper sheet protected the outermost layer. The 1 cm x 1 cm x 0.04 cm piezoceramic sheet had 13 stacked layers,

preloaded with a bolt and 1 kg mass. VPEEH experimental testing showed a useful output power of 1.23 mW to 1.64 mW at 33 Hz to 55 Hz, the operational frequency range. At 50 Hz, 5 g acceleration, and 200 kΩ load resistance, the maximum recorded voltage was 14 V. The highest output power observed was 4 mW at the same excitation, yielding 7.41 mW/cm<sup>3</sup> power density. Fig. 88 shows the suggested device schematic.

A non-linear wide-band VPEEH was proposed by Pertin et al. [131]. The suggested harvester had a 0.5 mm FR4 excised tapered guiding spring. A 3 mm x 0.2 mm PZT sheet was maintained by a spring at its fixed ends, and an 8 mm x 8 mm NdFeB proof mass lowered the resonance frequency. The system became non-linear when magnetic mass and spring were integrated due to spring stretching and bending. The VPEEH with a volume of 0.753 cm<sup>3</sup> was proposed. The detected power was 2600 μW with 0.9 g acceleration, 150 Hz frequency, 9 Hz bandwidth, and 4262.78 μW/cm<sup>3</sup>g<sup>2</sup> normalised power density. Fig. 89 shows the suggested device schematic.

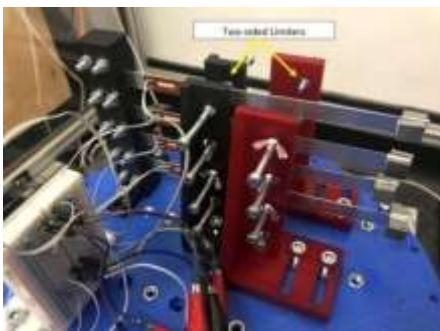


Fig. 87: Developed VPEEH [129]

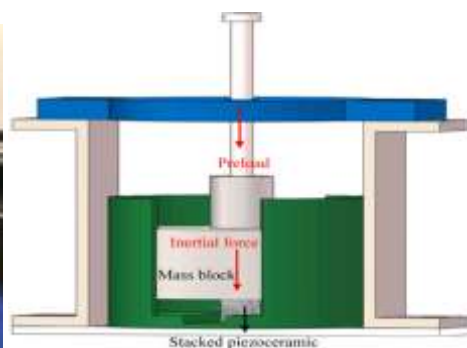


Fig. 88: Stacked-ceramic VPEEH [130]

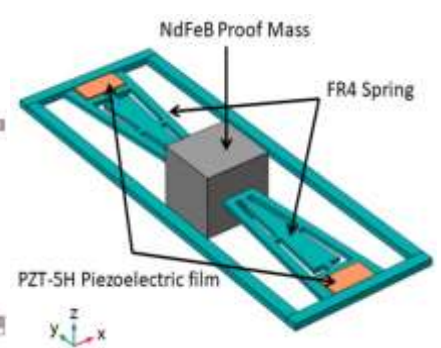


Fig. 89: Tapered VPEEH [131]

S.P. Machado et al. [132] produced a frequency-up-converting double impact unimorph VPEEH. The harvester had a driving beam, seismic mass, and 28 mm x 14 mm x 0.3 mm piezoelectric sheet. Dual impact produced an almost constant output voltage. The created beam limits large displacements and acts as an intrinsic brake for up and down motions, making the suggested device suitable for high acceleration applications. The harvester has a wide performance bandwidth and low optimum resistance. The gap, beam thickness, and tip mass were adjusted to improve the double impact frequency up-converting VPEEH's energy performance. Experiments with the harvester produced the highest power output of 1428  $\mu\text{W}$  at 20 Hz. For a frequency span of 17.5 Hz to 22 Hz, the average power was 400  $\mu\text{W}$ . Fig. 90 shows the gadget as designed.

A new dual-mode zigzag-shaped VPEEH runs on vibration and wind, according to Pan.] et al. [133]. This study introduced a zigzag energy harvester that can harvest wind and vibrational energy simultaneously. Fig. 91 showed a harvester with two beams: an inclined 85 mm x 15 mm x 0.7 mm beam and a horizontal 12 cm x 1.5 cm x 0.07 cm beam with a bluff body on the free end. The 15 cm x 4 cm x 4 cm bluff body stimulated wind flow-induced vibrations. It used a 2.5 cm x 1.5 cm x 0.03 cm piezoelectric patch to cover the slanted beam. Wind or base excitation distorted the piezoelectric patch, generating electricity. A pair of magnets added non-linearity to the system, expanding the operational

frequency bandwidth. The proposed hybrid harvester produced 10.1  $\mu\text{W}$  of electricity at 0.5 g and 14 Hz excitations. The voltage vs. frequency graph showed a 9-to-14-Hz frequency spectrum.

Han Yu et al. [134] developed a bird-shaped low-frequency wide-band VPEEH. Crossed elastic beams (beam M and W), PZT sheets, two counterweights (A and B), a proof mass, a pedestal, a support plate, rotating shafts, and wire made composed the harvester. Two PZT sheets were symmetrically affixed in series at each beam end, and a non-conductive glue bonded the cross beams. Supporting plates were on both sides of two spinning shafts that hinged beam W's ends. The supporting plate held counterweight B, which increased the harvester's productivity. To increase the operational frequency range, the proof mass should be positioned at the centre, while the counterweight must be located at the end of beam M. The introduction of the spinning shaft helped in lowering the harvester's intrinsic frequency. Modulating the output voltage of the harvester over numerous frequencies was made possible by combining proof mass with counterweights of varied specific gravities. The recommended VPEEH was experimentally assessed, providing power-out of 9.53 mW at 19.23 Hz vibration frequency and 1.83 mW at 45.38 Hz, with a baseline acceleration of 0.3 g. At this excitation level, the peak power density achieved was 19.85  $\mu\text{W}/\text{mm}^3$ . Fig. 92 shows the gadget.

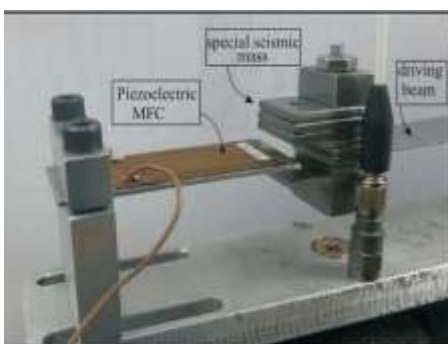


Fig. 90: FUC VPEEH [132]

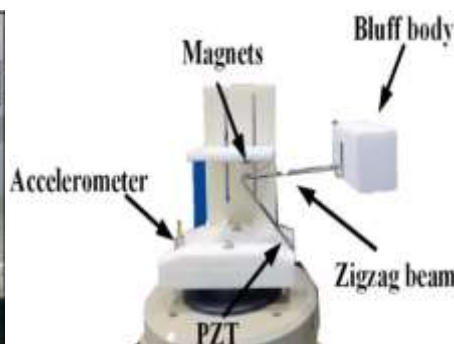


Fig. 91: Dual mode VPEEH [133]

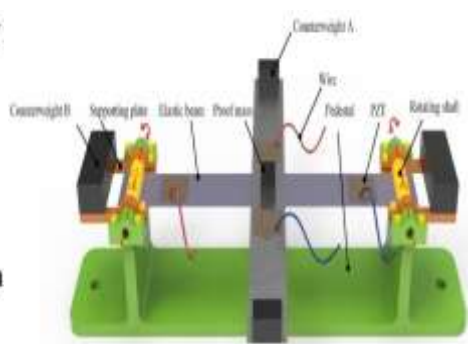


Fig. 92: Bird shaped VPEEH [134]

V. (C) COMPARISON OF THE REPORTED VPEEHs

This review compares VPEEHs based on device volume, vibration acceleration, operating frequency range, output

voltage, output power, and power density. Based on device parameters, Table V lists harvesters for comparison.

Table V: Comparative analysis of the reported VPEEHs

Type	Device Volume (cm <sup>3</sup> )	Acceleration (g)	Operating Frequency Range (Hz)	Frequency Bandwidth (Hz)	Voltage (mV)	Average Power Output (μW)	Power Density (μW/cm <sup>3</sup> )	Power / Acceleration (μW/g)	Power Density/Acceleration (μW/cm <sup>3</sup> g)	Ref.
Resonant	16.42 <sup>b</sup>	0.4	20.1	-	-	1530	93.2	3825	233	[114]
	-	2.5	25-41.4	16.4	3.3V	40	-	400	-	[115]
	1.99	0.5	50	-	56.1	240	120	480	240	[116]
	-	0.4 MPa Pressure	365 l/min air inflow	-	-	3410	-	-	-	[117]
	0.00042	1.5	-	406	5.36 V <sub>pp</sub>	7.182	17180	4.78	11454	[118]
	79.38 <sup>a</sup>	-	-	-	20V	43000	541.69	-	-	[119]
	0.00203 <sup>b</sup>	1.2	12.4 m/s velocity	-	1.88	0.9	443.8	0.75	369.83	[120]
	12.67 <sup>a</sup>	1	24	-	450	-	-	-	-	[121]
	0.0352 <sup>b</sup>	1	43.8	-	60.8V	380	10800	380	10800	[122]
Non-resonant	3.25	1	22-88	66	720	5.22	1.61	5.22	1.61	[123]
	4.335	-	7-13.5	6.5	-	825	190.3	-	-	[124]
	-	-	100-1000	130	160	20.5	-	-	-	[125]
	2.37 <sup>a</sup>	0.8	14-25	11	-	3400	1434	4250	1792	[126]
	3.9 <sup>a</sup>	1.5	117-123	6	-	321000	82307	214000	54871	[127]
	28	1	40-80	40	-	92200	3993	92200	3993	[128]
	4	0.2	5.7-12.3	6.6	1.7	6500	1625	32500	8125	[129]
	540 <sup>b</sup>	5	33-55	22	14	4000	7.41	800	1.482	[130]
	0.753	0.9	45-54	9	-	2600	3453	2889	3834	[131]
	-	-	17.5-22	4.5	-	400	-	-	-	[132]
	-	0.5	9-14	5	-	10.1	-	20.2	-	[133]
	0.48	0.3	19.2-45.3	26.1	-	5680	19850	18933	66166	[134]

Fig. 93 compares resonant and non-resonant harvesters by size and average power production. The harvester in [130] is the largest, non-resonant device with a volume of 540 cm<sup>3</sup> and a peak output power of 400 μW, resulting in a power density of 7.41 μW/cm<sup>3</sup>. The device reported in [118] is the smallest resonant device (0.00042 cm<sup>3</sup>) among VPEEHs, generating 7.18 μW of power with a power

density of 17180 μW/cm<sup>3</sup>. The greatest power is 321 mW from the non-resonant harvester in [127]. Power density vs. acceleration graph for reported VPEEHs is shown in Fig. 94. The non-resonant device in [127] has the lowest power density at 1.61 μW/cm<sup>3</sup>, while the device in [123] offers the maximum at 82307 μW/cm<sup>3</sup>. Non-resonant VPEEHs have a higher power density.

Fig. 95 compares VPEEH power per acceleration to device size. The harvester in [127], a non-resonant device, offers the most power per acceleration at 214000  $\mu\text{W}/\text{g}$ . The harvester in [120], a resonant device, has the lowest power per acceleration at 0.75  $\mu\text{W}/\text{g}$ . Fig. 95 shows that non-resonant VPEEHs have more power per acceleration than resonant.

Fig. 96 compares energy harvesting device frequency bandwidth and output power. According to reference

[125], the non-resonant broad band VPEEH operates at 130 Hz with a power output of 20.5  $\mu\text{W}$ . [132] describes a non-resonant device with a minimum frequency bandwidth of 4.5 Hz and a peak power-out of 400  $\mu\text{W}$ . The power vs frequency bandwidth graph shows that non-resonant VPEEHs have a wider frequency bandwidth than resonant.

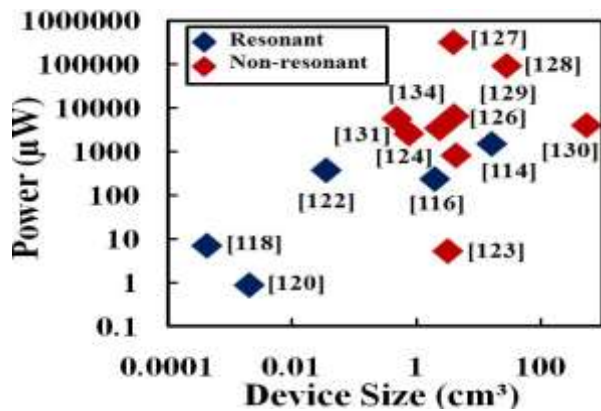


Fig. 93: Power vs. device volume of VPEEHs

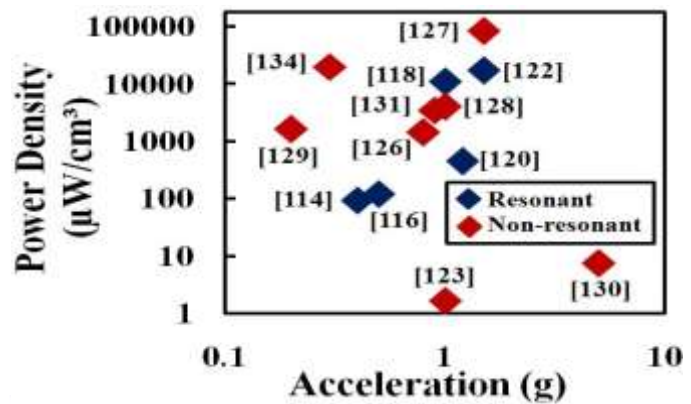


Fig.94: Power density vs. acceleration of VPEE

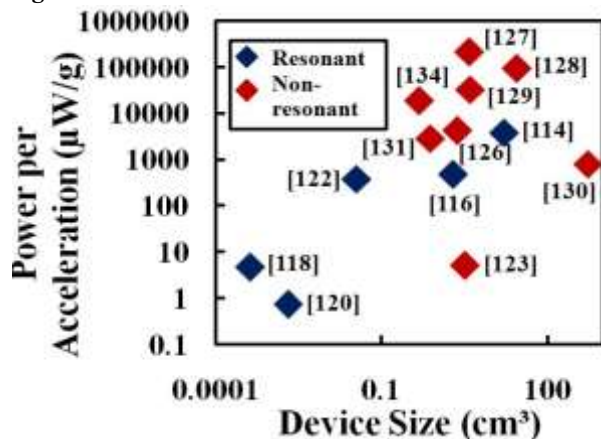


Fig. 95: Power per acceleration vs. size of the VPEEHs

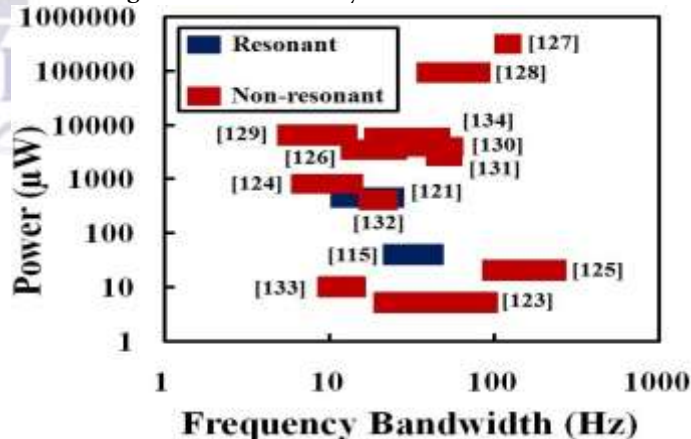


Fig. 96: The power vs. bandwidth of the VPEEHs

## VI. RESULTS

All reported energy harvesters are evaluated for six essential parameters: operating frequencies range, harvester size, power output, operational acceleration, power-to-acceleration ratio, and power density.

### 1. Operational frequency range

The typical operating frequency for VEMEHS is 1-100 Hz.

VESEHS perform effectively at 10-1000 Hz.

VPEEHs operate from 1-1000 Hz.

### 2. Harvester size

VEMEHS range from 0.032 to 1600  $\text{cm}^3$ .

VESEHS range from 0.0025 to 2.25  $\text{cm}^3$ .

VPEEHs range from 0.00042 to 540  $\text{cm}^3$ .

### 3. Power output

The power output range of VEMEHS is 0.00096  $\mu\text{W}$  to 74,000  $\mu\text{W}$ .

VESEHS are picowatts to 600 microwatts.

Range of VPEEHs: 0.9  $\mu\text{W}$  to 321 mW.

**4. Acceleration**

For VEMEHs, acceleration is usually 0.1-10 g.  
 VESEHs need 1-100 g acceleration.  
 VPEEHs can support 10-1000 g accelerations.

**5. Power per acceleration**

VEMEHs range from  $0.016 \times 10^3 \mu\text{W/g}$  to  $129.8 \text{ mW/g}$ .  
 VESEHs range from 0.082 to  $81.76 \mu\text{W/g}$ .  
 VPEEHs have a power range of 0.75 to  $214,000 \mu\text{W/g}$ .

**6. Power density**

VEMEHs have a power range of  $5 \times 10^7$  to  $1073 \mu\text{W/cm}^3$ .  
 VESEHs range from 0.52 to  $19616 \mu\text{W/cm}^3$ .  
 VPEEHs show a range of 1.61 to  $82,307 \mu\text{W/cm}^3$ .  
 Comparative investigation demonstrates that VPEEHs are the best vibration energy collector because they have a wide range of operational frequencies, a better power-to-acceleration ratio, and higher power output and density for high acceleration.  
 VEMEHs and VESEHs have their advantages, but VPEEHs seem to give the best performance and versatility. Use and needs will determine the harvester.

**VII. CONCLUSION**

Remote wireless sensor nodes increasingly need vibration-based energy harvesters (VEHs). VPEEHs outperform electrostatic (VEMEH), piezoelectric (VPEEH), and electromagnetic (VEMEH). Wide working frequency ranges, better power output, power density, and superior power-to-acceleration ratios. Resonant VEHs are larger and less bandwidth-efficient but produce more power. But non-resonant VEHs are better at frequency bandwidth. Comparative investigation across six important characteristics shows VPEEHs are the most promising vibration energy harvesting option, although the best choice is application-specific.

**REFERENCES**

E. M. Yeatman, "Energy scavenging for wireless sensor nodes," in Proceedings of the 2nd International Workshop on Advances in Sensors and Interfaces, Bari, Italy, pp.1-4, June 2007, <https://DOI.10.1109/IWASI.2007.4420014>  
 Khan, F.U., Review of non-resonant vibration based energy harvesters for wireless sensor nodes. Journal of Renewable and Sustainable Energy,

vol. 8, no. 4, 2016, <https://doi.org/10.1063/1.4961370>

Texas Instruments for description and information of analog output temperature sensor (Online) Available at: [www.ti.com/LMT85](http://www.ti.com/LMT85)(accessed: May 10, 2019).

Microchip for data sheet and specifications of temperature sensor model MCP9701A, (Online) Available at: [www.microchip.com/wwwproducts/en/MCP9701A](http://www.microchip.com/wwwproducts/en/MCP9701A) MCP9701A (accessed May 10, 2019).

Microchip for data sheet and specifications of temperature sensor model MCP9700(Online) Available

at:[www.microchip.com/wwwproducts/en/MCP9700](http://www.microchip.com/wwwproducts/en/MCP9700) (accessed May 10, 2019)

Analog devices for datasheet and product info of voltage output temperature sensor TMP35 (Online) Available at:

[www.analog.com/TMP35](http://www.analog.com/TMP35)(accessed May 10, 2019)

Smart sensor solutions for info of digital temperature sensor model STS3x (Online) Available at: [www.sensirion.com/STS3x](http://www.sensirion.com/STS3x)(accessed May 10, 2019)

Texas instruments for data sheet of digital output temperature sensor TMP 101 (Online) Available at: [www.ti.com/TMP101](http://www.ti.com/TMP101) (accessed May 10, 2019)

Made in China for data sheet and specifications of pressure sensor model QYK (Online) available at: [www.leiliyk.en.made-in-china.com](http://www.leiliyk.en.made-in-china.com)(accessed June 4, 2019)

TE Connectivity for pressure sensor details, (Online) Available at: [www.te.com/usa-en/product-CAT-BLPS0002](http://www.te.com/usa-en/product-CAT-BLPS0002) (accessed June 4, 2019)

Made in China for pressure sensor details (Online) Available at: <https://micorsensor.en.made-in-china.com/product/USdQXArVEwcW/China-19mm-OEM-Compact-Cost-Effective-Pressure-Sensor-Mpm286>(accessed June 4, 2019)

Made in China, (Online) Available at: <https://tmsensor.en.made-in-china.com/product/VXyndGIjQvkC/China-Pressure-Sensor-Ns-P22-Pressure-Transmitter-Pressure-Transducer.html>(accessed June 4, 2019)

- Analog devices, for specifications of acceleration sensor ADXL103/ ADXL 203 (Online) Available at: [www.analog.com/accelerometers/adxl103.html](http://www.analog.com/accelerometers/adxl103.html)(accessed June 4, 2019)
- Analog devices for specifications of acceleration sensor ADXL1357 (Online) Available at: [www.analog.com/en/products/mems/accelerometers/adxl1357](http://www.analog.com/en/products/mems/accelerometers/adxl1357)(accessed June 4, 2019)
- Analog devices for specifications of acceleration sensor ADXL1357 (Online) Available at: [www.analog.com/en/products/mems/accelerometers/adxl251](http://www.analog.com/en/products/mems/accelerometers/adxl251)(accessed June 4, 2019)
- Texas Instruments for specifications of acceleration sensor model:DRV-ACC16-EVM (Online) Available at: [www.ti.com/tool/drv-acc16-evm](http://www.ti.com/tool/drv-acc16-evm)(accessed June 4, 2019)
- STMicroelectronics for inertial sensor data sheet (Online) Available at: <https://www.st.com/resource/en/datasheet/cd00068496.pdf>(accessed June 4, 2019)
- Turbo Future for idea about batteries specifications, (Online) Available at: [www.turbofuture.com/misc/Know-What-Type-of-Battery-to-Use-in-Equipment](http://www.turbofuture.com/misc/Know-What-Type-of-Battery-to-Use-in-Equipment)(accessed June 14, 2019)
- Battery University for general idea about batteries specifications, (Online) Available at: [https://batteryuniversity.com/learn/archive/whats\\_the\\_best\\_battery](https://batteryuniversity.com/learn/archive/whats_the_best_battery)(accessed June 14,2019)
- D. Upadrashta, Y. Yang, "Nonlinear piezomagnetoelastic harvester array for broadband energy harvesting", J. Appl.Phys. Vol.120, no.5, Aug 2016, <https://doi.org/10.1063/1.4960442>
- L.H. Tang, Y.W. Yang, C.K. Soh, "Toward broadband vibration based energy harvesting", J. Intell. Mater. Syst. Struct. Vol. 21, no.18, pp. 1867-1897,Dec, 2010, <https://doi.org/10.1177/1045389X10390249>.
- Y. Wu, H. Ji, J. Qiu, L. Han, "A 2-degree-of-freedom cubic nonlinear piezoelectric harvester intended for practical low-frequency vibration", Sensors And Actuators, A: Physical 264, pp.1-10, Sept 2017, <https://doi.org/10.1016/j.sna.2017.06.029>
- D. Isarakorn, D. Briand, P. Janphuang, A. Sambri, S. Gariglio, J.-M. Triscone , F. Guy , J. W. Reiner , C. H. Ahn, N. F. de Rooij "Energy harvesting MEMS device based on an epitaxial PZT thin film: Fabrication and characterization", Power MEMS Tech. Dig.pp.203 - 206, 2010.
- Paul D. Mitcheson, Tim C. Green. "Maximum Effectiveness of Electrostatic Energy Harvester When Coupled to Interface Circuits", IEEE Trans. on Circuits and Systems vol. 59, no. 12, pp. 3098-3111 2012, <https://DOI.10.1109/TCSI.2012.2206432>
- Wang P, Li W, Che L, "Design and fabrication of a micro electromagnetic vibration energy harvester". J Semicondv.10, no.1, pp.1 - 4, 2012, <https://DOI.10.1088/1674-4926/32/10/104009>
- M. F. Bin Ab Rahman and K. S. Leong, "Investigation of useful ambient vibration sources for the application of energy harvesting," in Proceedings of the IEEE Student Conference on Research and Development (SCOREd),Vol. 19-20, pp. 391-396, 2011, <https://DOI.10.1109/SCOREd.2011.6148771>
- M. F. Bin Ab Rahman and K. S. Leong, "Investigation of useful ambient vibrationsources for the application of energy harvesting," in Proceedings of the IEEE Student Conference on Research and Development (SCOREd) , vol.19- 20, pp. 391-396, 2011, <https://DOI.10.1109/SCOREd.2011.6148771>
- Gao and Y. Cui, "Vibration-based sensor powering for manufacturing process monitoring," Trans. North Am. Manuf. Res. Inst. Soc. Manuf. Eng. Vol. 33, pp.335-342, 2005.
- Gulf coast data for vibration analysis using an X6-2 USB accelerometer (Online) Available at: [http://www.gcdataconcepts.com/ac\\_vibration.html](http://www.gcdataconcepts.com/ac_vibration.html)(accessed July 9, 2019).
- Holistic energy harvesting, for vibration data of domestic washing machine and general information, (Online) Available at: [http://www.holistic.ecs.soton.ac.uk/data/home\\_washing/data.php](http://www.holistic.ecs.soton.ac.uk/data/home_washing/data.php)(accessed July 10, 2019).

- Bateman VI. MIL-STD-810G, Change 1 Accelerometer Requirements for Shock. Sound & Vibration. 2014 Apr 1:5
- S. Gnanasekaran, M. Ajovalasit, and J. Giacomini, "Driver estimation of steering wheel vibration intensity: Laboratory based tests," *Engineering Integrity* vol. 20, no.1, pp.25-31, 2006, <https://doi.org/10.1002/pts.955>
- V. Chonhenchob, S. P. Singh, J. J. Singh, J. Stallings, and G. Grewal, "Measurement and analysis of vehicle vibration for delivering packages in small-sized and medium-sized trucks and automobiles," *Packag. Technol. Sci.* vol.25, pp.31-38, 2012, <https://doi.org/10.1002/pts.955>
- Q. Zhu, M. Quan, and Y. He, "Vibration energy harvesting in automobiles to power wireless sensors," in *Proceedings of the International Conference on Information and Automation (ICIA 2012)*, Shenyang, Liaoning, China, pp.349-354, 2012, <https://DOI.10.1109/ICInfA.2012.6246873>
- T. Irvine, *Welcome to vibration data*, (Online) Available at: [http://www.vibrationdata.com/Newsletters/August2004\\_NL.pdf](http://www.vibrationdata.com/Newsletters/August2004_NL.pdf) (accessed July 21, 2019)
- Bendame M and Abdel-Rahman E M 2012 Nonlinear modeling and analysis of a vertical springless energy harvester *Int. Conf. on Structural Nonlinear Dynamics and Diagnosis (CSNDD)*, Morocco, pp.1 01-104, 2012, <https://doi.org/10.1051/mateconf/20120101004>
- Bendame, Mohamed, Eihab Abdel-Rahman, and Mostafa Soliman. "Test and validation of a nonlinear electromagnetic energy harvester." In *International Design Engineering Technical Conferences and Computers and Information in Engineering Conference*, vol. 46353, p. V004T09A030. American Society of Mechanical Engineers, 2014, <https://doi.org/10.1051/mateconf/20120101004>
- Bedekar V, Oliver J and Priya S, Pen harvester for powering a pulse rate sensor *J. Phys. D: Appl. Phys.* 42 105105, 2009, <https://doi.10.1088/0022-3727/42/10/105105>
- Mohamed M A, Abdel-Rahman E M, Mansour R R and El-Saadany E F "Springless vibration energy harvesters" *American Society of Mechanical Engineers IDETC (Montréal, Canada)* vol. 4, pp. 703-11, 2010, <https://doi.org/10.1115/DETC2010-29046>
- Joyce B S, Farmer J and Inman D J " Electromagnetic energy harvester for monitoring wind turbine blades" *Wind Energy*, vol. 17 pp. 869-76, 2014, <https://doi.org/10.1002/we.1602>
- Roundy, Shad, Paul K. Wright, and Jan Rabaey. "A study of low level vibrations as a power source for wireless sensor nodes." *Computer communications*, vol. 26, no. 11, 2003, [https://doi.org/10.1016/S0140-3664\(02\)00248-7](https://doi.org/10.1016/S0140-3664(02)00248-7)
- Mitcheson, Paul D., Tim C. Green, Eric M. Yeatman, and Andrew S. Holmes. "Architectures for vibration-driven micropower generators." *Journal of microelectromechanical systems* vol. 13, no. 3, pp. 429-440, 2004, <https://DOI.10.1109/JMEMS.2004.830151>
- Anton, Steven R., and Henry A. Sodano. "A review of power harvesting using piezoelectric materials (2003-2006)." *Smart materials and Structures* vol. 16, no. 3, 2007, <https://DOI.10.1088/0964-1726/16/3/R01>
- El-Hami, M., Glynne-Jones, P., White, N.M., Hill, M., Beeby, S., James, E., Brown, A.D. and Ross, J.N., Design and fabrication of a new vibration-based electromechanical power generator. *Sensors and Actuators A: Physical*, vol.92, no.1-3, pp.335-342, 2001, [https://doi.org/10.1016/S0924-4247\(01\)00569-6](https://doi.org/10.1016/S0924-4247(01)00569-6)
- Roundy, Shad, and Yang Zhang. "Toward self-tuning adaptive vibration-based microgenerators." In *Smart structures, devices, and systems II*, vol. 5649, pp. 373-384. SPIE, 2005, <https://doi.org/10.1117/12.581887>
- Wu, X., Lin, J., Kato, S., Zhang, K., Ren, T. and Liu, L., A frequency adjustable vibration energy harvester. *Proceedings of Power MEMS*, pp.245-248, 2008.
- Challa, Vinod R., Marehalli G. Prasad, Yong Shi, and Frank T. Fisher. "A vibration energy harvesting device with bidirectional resonance frequency tunability." *Smart Materials and Structures* vol.

- 17, no. 1, pp.015-035, 2008, <https://doi.org/10.1016/j.sna.2013.09.015>
- H. C. Liu, Y. Qian, and C. K. Lee, "A multi-frequency vibration-based MEMS electromagnetic energy harvesting device," *Sens. Actuators A, Phys.*, vol. 204, pp. 37-43, 2013, <https://doi.org/10.1016/j.sna.2013.09.015>
- S. P. Beeby et al., "A micro electromagnetic generator for vibration energy harvesting" *J.Micromech. Microeng.* vol. 17, pp. 1257-1265, 2007, DOI 10.1088/0960-1317/17/7/007.
- S. D. Kwon, J. Park, and K. Law, "Electromagnetic energy harvester with repulsively stacked multilayer magnets for low frequency vibrations" *Smart Mater. Struct.*, vol. 22, no. 5, p. 055007, 2013, <https://DOI.10.1088/0964-1726/22/5/055007>
- Heit, John, David Christensen, and Shad Roundy. "A vibration energy harvesting structure, tunable over a wide frequency range using minimal actuation." In *Smart Materials, Adaptive Structures and Intelligent Systems*, vol. 56048, p. V002T07A017. American Society of Mechanical Engineers, 2013, <https://doi.org/10.1115/SMASIS2013-3165>
- Takahiro Sato, Kota Watanabe and Hajime Igarashi "Coupled Analysis of Electromagnetic Vibration Energy Harvester With Nonlinear Oscillation" *IEEE Transaction on Magnetics*, vol. 50, no. 2, Feb 2014, <https://DOI.10.1109/TMAG.2013.2284253>
- Podder, Pranay, Andreas Amann, and Saibal Roy. "Combined effect of bistability and mechanical impact on the performance of a nonlinear electromagnetic vibration energy harvester." *IEEE/ASME Transactions On Mechatronics*, vol. 21, no. 2, pp. 727-739, 2016, <https://DOI.10.1109/TMECH.2015.2451016>
- Xing, X., J. Lou, G. M. Yang, O. Obi, C. Driscoll, and N. X. Sun. "Wideband vibration energy harvester with high permeability magnetic material." *Applied Physics Letters* vol. 95, no. 13, 2009; <https://doi.10.1063/1.3238319>
- R. Paul and B. George "Automatic flipping magnet type electromagnetic energy harvester" *ELECTRONICS LETTERS*, vol. 52, no. 17 pp. 1476-1478, 2016, <https://doi.org/10.1049/el.2016.1103>
- Park, Jinkyoo, Soonduck Kwon, and Kincho H. Law. "Asynchronous phase shifted electromagnetic energy harvester." In *Sensors and Smart Structures Technologies for Civil, Mechanical, and Aerospace Systems*, vol. 8692, pp. 399-411. SPIE, 2013, <https://doi.org/10.1117/12.2009615>
- Soliman, M. S. M., E. F. El-Saadany, E. M. Abdel-Rahman, and R. R. Mansour. "Design and modeling of a wideband MEMS-based energy harvester with experimental verification." In *2008 1st Microsystems and Nanoelectronics Research Conference*, pp. 193-196. IEEE, 2008, <https://DOI.10.1109/MNRC.2008.4683411>
- B. Yang et al., "Electromagnetic energy harvesting from vibrations of multiple frequencies," *J. Micromech. Microeng.*, vol. 19, no. 3, p. 035001, 2009, <https://DOI.10.1088/0960-1317/19/3/035001>
- I. Sari, T. Balkan, and H. Kulah, "An electromagnetic micro power generator for wideband environmental vibrations," *Sensors Actuat. A, Phys.*, vols. 145-146, pp. 405-413, 2008, <https://doi.org/10.1016/j.sna.2007.11.021>
- H. Liu, T. Chen, L. Sun, and C. Lee, "An electromagnetic MEMS energy harvester array with multiple vibration modes," *Micromachines*, vol. 6, no. 8, pp. 984-992, 2015, <https://doi.org/10.3390/mi6080984>
- K. Tao et al., "A novel two-degree-of-freedom MEMS electromagnetic vibration energy harvester," *J. Micromech. Microeng.*, vol. 26, no. 3, p. 035020, 2016, <https://DOI.10.1088/0960-1317/26/3/035020>
- Fan, K., Cai, M., Liu, H. and Zhang, Y., "Capturing energy from ultra-low frequency vibrations and human motion through a monostable electromagnetic energy harvester". *Energy*, vol. 169, pp.356-368, 2019, <https://doi.org/10.1016/j.energy.2018.12.053>
- Shahosseini, Iman, Rebecca L. Peterson, Ethem E. Aktakka, and Khalil Najafi. "Electromagnetic generator optimization for non-resonant energy harvester." In *SENSORS, 2014 IEEE*, pp. 178-181. IEEE, 2014, <https://DOI.10.1109/ICSENS.2014.6984962>

- Galchev, T., Kim, H. and Najafi, K., Micro power generator for harvesting low-frequency and nonperiodic vibrations. *Journal of Microelectromechanical Systems*, vol. 20, no. 4, pp.852-866, 2011, <https://DOI.10.1109/JMEMS.2011.2160045>
- Yeo, Jeongjin, Heajeong Park, Jonghyun Jo, and Yoonseok Yang. "Multi-dimensional vibration energy harvester for efficient use in common environment." In 2015 IEEE SENSORS, pp. 1-4. IEEE, 2015, <https://DOI.10.1109/ICSENS.2015.7370469>
- Yang, Bin, and Chengkuo Lee. "Non-resonant electromagnetic wideband energy harvesting mechanism for low frequency vibrations." *Microsystem Technologies* vol. 16 pp. 961-966, 2010, <https://doi.10.1007/s00542-010-1059-z>
- Bradai, S., Naifar, S., Viehweger, C., Kanoun, O. and Litak, G., Nonlinear analysis of an electrodynamic broadband energy harvester. *The European Physical Journal Special Topics*, vol. 224, pp.2919-2927, 2015. <https://doi.10.1140/epjst/e2015-02598-0>
- Kangqi Fan, Yiwei Zhang, Haiyan Liu, Meiling Cai, Qinxue Tan "A nonlinear two-degree-of-freedom electromagnetic energy harvester for ultra-low frequency vibrations and human body motions" *Renewable Energy* vol. 138, pp.292-302, 2019, <https://doi.org/10.1016/j.renene.2019.01.105>
- O. Zorlu and H. Kulah, "A miniature and non-resonant vibration-based energy harvester structure," in *Proceedings of the 26th European Conference on Solid-State Transducers (EUROSENSOR 2012)*, Poland Vol. 47, pp.664-667, 2012, <https://doi.org/10.1063/1.4867216>
- M. A. Halim and J. Y. Park, "A non-resonant, frequency up-converted electromagnetic energy harvester from humanbody-induced vibration for hand-held smart system applications," *J. Appl. Phys.* 115, 094901, 2014, <https://doi.org/10.1063/1.4867216>
- Li, X., T. Hehn, M. Thewes, I. Kuehne, Alexander Frey, G. Scholl, and Y. Manoli. "Non-resonant electromagnetic energy harvester for car-key applications." In *Journal of Physics: Conference Series*, vol. 476, no. 1, p. 012096. IOP Publishing, 2013, <https://DOI.10.1088/1742-6596/476/1/012096>
- Bowers, B.J. and Arnold, D.P., Spherical magnetic generators for bio-motional energy harvesting. *Proceedings of PowerMEMS*, pp.281-284, 2008.
- M. Han, W. Liu, B. Meng, X.-S. Zhang, X. Sun, and H. Zhang, "Springless cubic harvester for converting three dimensional vibration energy," in *Proc. IEEE 27th Int. Conf. Micro Electro Mech. Syst. (MEMS)*, pp. 425-428, Jan. 2014, <https://DOI.10.1109/MEMSYS.2014.6765667>
- Kurt, E., Issimova, A. and Medetov, B., A wide-band electromagnetic energy harvester. *Energy*, 277, p.127693, 2023, <https://doi.org/10.1016/j.energy.2023.127693>
- Shen, Y. and Lu, K., Scavenging power from ultra-low frequency and large amplitude vibration source through a new non-resonant electromagnetic energy harvester. *Energy Conversion and Management*, 222, p.113233, 2020, <https://doi.org/10.1016/j.enconman.2020.113233>
- J. Zhang and Y. Su, Design and analysis of a non-resonant rotational electromagnetic harvester with alternating magnet sequence, *Journal of Magnetism and Magnetic Materials*, 540, p.168393, 2021, <https://doi.org/10.1016/j.jmmm.2021.168393>
- K. Krzysztof and E. Stezycka. "Nonlinear Dynamics and Energy Harvesting of a Two-Degrees-of-Freedom Electromagnetic Energy Harvester near the Primary and Secondary Resonances." *Applied Sciences* vol. 13, no. 13, p.7613, 2023, <https://doi.org/10.3390/app13137613>
- Holm, P., Imbaquingo, C., Mann, B.P. and Bjørk, R., High power electromagnetic vibration harvesting using a magnetic dumbbell structure. *Journal of Sound and Vibration*, 546, p.117446, 2023, <https://doi.org/10.1016/j.jsv.2022.117446>
- Jeong, S.Y., Liu, W.C., Cho, J.Y., Oh, Y.J., Kumar, A., Woo, S.B., Do Hong, S., Ryu, C.H. and Sung, T.H., A sustainable self-generating system driven by human energy for wearable safety solutions. *Energy Conversion and Management: X*, 23, p.100667, 2024, <https://doi.org/10.1016/j.ecmx.2024.100667>

- Li, G., Zhang, X. and Su, S., Dynamic modeling and experimental study of multi-coil composite core energy harvester. *Sensors and Actuators A: Physical*, 369, p.115198, 2024, <https://doi.org/10.1016/j.sna.2024.115198>
- Nicolini, L. and Castagnetti, D., A wideband low frequency 3D printed electromagnetic energy harvester based on orthoplanar springs. *Energy Conversion and Management*, 300, p.117903, 2024, <https://doi.org/10.1016/j.enconman.2023.117903>
- Royo-Silvestre, I., Beato-López, J.J. and Gómez-Polo, C., Optimization procedure of low frequency vibration energy harvester based on magnetic levitation. *Applied Energy*, 360, p.122778, 2024, <https://doi.org/10.1016/j.apenergy.2024.122778>
- Wang, L., Liu, T., Hao, G., Chitta, S., Liu, L., Ye, T., Zhang, Z. and Wang, N., An electromagnetic vibration energy harvester with compact flexure guide for low frequency applications. *Smart Materials and Structures*, 33(1), p.015031, 2023, <https://doi.org/10.1088/1361-665X/ad1429>
- Pan, X., Zhang, G., Yu, N., Cai, C., Ma, H. and Yan, B., Low-frequency human motion energy scavenging with wearable tumbler-inspired electromagnetic energy harvesters. *International Journal of Mechanical Sciences*, 268, p.109029, 2024, <https://doi.org/10.1016/j.ijmecsci.2024.109029>
- Rajarithnam, M., Awrejcewicz, J. and Ali, S.F., A novel design of an array of pendulum-based electromagnetic broadband vibration energy harvester. *Mechanical Systems and Signal Processing*, 208, p.110955, 2024, <https://doi.org/10.1016/j.ymsp.2023.110955>
- Iannacci, Jacopo, Guido Sordo, Massimo Gottardi, Thomas Kuenzig, Gabriele Schrag, and Gerhard Wachutka. "An Energy Harvester concept for electrostatic conversion manufactured in MEMS surface micromachining technology." In 2013 International Semiconductor Conference Dresden-Grenoble (ISCDG), pp. 1-4. IEEE, 2013. <https://doi.org/10.1109/ISCDG.2013.6656310>
- Renaud, Michael, Geert Altena, Martijn Goedbloed, Christine de Nooijer, Svetlana Matova, Y. Naito, T. Yamakawa, H. Takeuchi, K. Onishi, and Rob van Schaijk. "A high performance electrostatic MEMS vibration energy harvester with corrugated inorganic SiO<sub>2</sub>-Si<sub>3</sub>N<sub>4</sub> electret." In 2013 Transducers & Eurosensors XXVII: The 17th International Conference on Solid-State Sensors, Actuators and Microsystems (TRANSDUCERS & EUROSENSORS XXVII), pp. 693-696. IEEE, 2013. <https://doi.org/10.1109/Transducers.2013.6626861>
- Michail E. Kiziroglou, Cairan He, and Eric M. Yeatman "Rolling Rod Electrostatic Microgenerator" *IEEE TRANSACTIONS ON INDUSTRIAL ELECTRONICS*, VOL. 56, NO. 4, APRIL 2009. <https://doi.org/10.1109/TIE.2008.2004381>
- Torres, Erick O., and Gabriel A. Rincon-Mora. "Electrostatic energy harvester and Li-Ion charger circuit for micro-scale applications." In 2006 49th IEEE International Midwest Symposium on Circuits and Systems, vol. 1, pp. 65-69. IEEE, 2006. <https://doi.org/10.1109/MWSCAS.2006.381996>
- Bu, Ling, Huiyong Xu, and Bingji Xu. "A novel electrostatic vibration energy harvester array using sidewall electric field." In 2014 12th IEEE International Conference on Solid-State and Integrated Circuit Technology (ICSICT), pp. 1-3. IEEE, 2014. <https://doi.org/10.1109/ICSICT.2014.7021222>
- Kim, Dongil, Seonuk Yu, Byeong-Geun Kang, and Kwang-Seok Yun. "Electrostatic energy harvester using magnetically actuated liquid dielectric layers." *Journal of Microelectromechanical Systems* 24, no. 3, pp. 516-518, 2015. <https://doi.org/10.1109/JMEMS.2015.2413811>
- Kiziroglou, M. E., C. He, and E. M. Yeatman. "Flexible substrate electrostatic energy harvester." *Electronics letters* 46, no. 2, pp. 166-167, 2010. <https://doi.org/10.1049/el.2010.2462>
- Seo, Min-Ho, Dong-Hoon Choi, Chang-Hoon Han, Jae-Young Yoo, and Jun-Bo Yoon. "An electrostatic energy harvester exploiting variable-area water electrode by respiration." In 2015 28th IEEE

- International Conference on Micro Electro Mechanical Systems (MEMS), pp. 126-129. IEEE, 2015. <https://DOI.10.1109/MEMSYS.2015.7050902>
- Fowler, A.G., Moheimani, S.R. and Behrens, S., Design and characterization of a 2-DOF MEMS ultrasonic energy harvester with triangular electrostatic electrodes. IEEE electron device letters, 34(11), pp.1421-1423, 2013. <https://DOI.10.1109/LED.2013.2282815>
- Suzuki, Takafumi, Sumito Nagasawa, Hiroshi Okamoto, and Hiroki Kuwano. "Novel vibration-driven micro-electrostatic induction energy harvester with asymmetric multi-resonant spring." In SENSORS, 2010 IEEE, pp. 1161-1164. IEEE, 2010. <https://DOI.10.1109/ICSENS.2010.5690694>
- Kim, Sehwan, Sungil Bang, and Kukjin Chun. "Temperature effect on the vibration-based electrostatic energy harvester." In TENCON 2011-2011 IEEE Region 10 Conference, pp. 1317-1320. IEEE, 2011. <https://DOI.10.1109/TENCON.2011.6129021>
- Ahmad, Mohamad Radzi Bin, and Mohd Haris Bin Md Khir. "Design, analysis and fabrication of Electret-based micro-electromechanical systems energy harvester." In 2011 National Postgraduate Conference, pp. 1-4. IEEE, 2011. <https://DOI.10.1109/NatPC.2011.6136424>
- Guillemet, R., Philippe Basset, Dimitri Galayko, Francesco Cottone, Frédéric Marty, and Tarik Bourouina. "Wideband MEMS electrostatic vibration energy harvesters based on gap-closing interdigitated combs with a trapezoidal cross section." In 2013 IEEE 26th International Conference on Micro Electro Mechanical Systems (MEMS), pp. 817-820. IEEE, 2013. <https://DOI.10.1109/MEMSYS.2013.6474368>
- Abdulmunam, R. T., L. Y. Taha, and P. C. Ivey. "Simulink model of an integrated rotary electrostatic energy harvester." In 2012 13th International Conference on Optimization of Electrical and Electronic Equipment (OPTIM), pp. 1006-1011. IEEE, 2012. <https://DOI.10.1109/OPTIM.2012.6231820>
- Pondrom, P., G. M. Sessler, J. Bös, and Tobias Melz. "Compact electret energy harvester with high power output." Applied Physics Letters 109, no. 5, 2016. <https://doi.org/10.1063/1.4960480>
- Lu, Yingxian, Francesco Cottone, Sébastien Boisseau, Frédéric Marty, Dimitri Galayko, and Philippe Basset. "Low-frequency and ultra-wideband MEMS electrostatic vibration energy harvester powering an autonomous wireless temperature sensor node." In 2016 IEEE 29th International Conference on Micro Electro Mechanical Systems (MEMS), pp. 33-36. IEEE, 2016. <https://DOI.10.1109/MEMSYS.2016.7421550>
- Ramadan, Khaled, and Ian G. Foulds. "Fabrication of SU-8 low frequency electrostatic energy harvester." In 2011 International Conference on Energy Aware Computing, pp. 1-5. IEEE, 2011. <https://DOI.10.1109/ICEAC.2011.6136689>
- Zhang, Ai, Zhuoteng Peng, Anxin Luo, Shanshan Li, and Fei Wang. "Electrostatic energy harvesting device with broad bandwidth." In 2015 International Conference on Manipulation, Manufacturing and Measurement on the Nanoscale (3M-NANO), pp. 178-181. IEEE, 2015. <https://DOI.10.1109/3M-NANO.2015.7425489>
- Bu, Ling, Xiaoming Wu, Xiaohong Wang, and Litian Liu. "Non-resonant electrostatic energy harvester for wideband applications." Micro & Nano Letters vol. 8, no. 3, pp. 135-137, 2013. <https://doi.org/10.1049/mnl.2012.0924>
- Nguyen, S.D., Halvorsen, E. and Jensen, G.U., Wideband MEMS energy harvester driven by colored noise. Journal of microelectromechanical systems, vol. 22no. 4, pp.892-900, 2013. <https://DOI.10.1109/JMEMS.2013.2248343>
- Tao, K., S. W. Liu, J. M. Miao, and S. W. Lye. "A three-dimensional electrostatic/electret micro power generator for low acceleration and low frequency vibration energy harvesting." In 2014 IEEE 27th International Conference on Micro Electro Mechanical Systems (MEMS), pp. 366-369. IEEE, 2014. <https://DOI.10.1109/MEMSYS.2014.6765652>

- Pourahmadi-Nakhli, Meisam, Bahareh Sasanpour, Mostafa Mahdavi, and Mohsen Sharifpur. "Optimal heartbeat energy harvesting using electrostatic energy harvesters." *Energy Technology* 11, no. 11 2023, <https://doi.org/10.1002/ente.202300569>
- Zhang, Y., Wang, T., Luo, A., Hu, Y., Li, X. and Wang, F., 2018. Micro electrostatic energy harvester with both broad bandwidth and high normalized power density. *Applied energy*, 212, pp.362-371. <https://doi.org/10.1016/j.apenergy.2017.12.053>
- Yamane, Daisuke, Kentaro Tamura, Keigo Nota, RyutaIwakawa, Cheng-Yao Lo, Kazumoto Miwa, and Shimpei Ono. "Contactless Electrostatic Vibration Energy Harvesting Using Electric Double Layer Electrets." *Sensors & Materials* 34, 2022. <https://doi.org/10.18494/SAM3945>
- Vysotskyi, B., Campos, J.F.A., Lefevre, E. and Brenes, A., Dynamic analysis of a novel two-sided nonlinear MEMS electrostatic energy harvester. *Mechanical Systems and Signal Processing*, 206, p.110932, 2024. <https://doi.org/10.1016/j.ymsp.2023.110932>
- Honma, Hiroaki, Yukiya Tohyama, and Hiroshi Toshiyoshi. "A short-stroke electrostatic vibrational energy harvester with extended bandwidth and sensitivity." In 2021 21st International Conference on Solid-State Sensors, Actuators and Microsystems (Transducers), pp. 132-135. IEEE, 2021. <https://doi.org/10.1109/Transducers50396.2021.9495535>
- Li, M., Luo, A., Luo, W., Liu, X. and Wang, F., Electrostatic vibration energy harvester with a self-rechargeable electret. *IEEE Electron Device Letters*, 44(3), pp.540-543, 2023. <https://DOI.10.1109/LED.2023.3240836>
- Kim, Sang-Gook, Shashank Priya, and Isaku Kanno. "Piezoelectric MEMS for energy harvesting." *MRS bulletin* 37, no. 11, pp. 1039-1050, 2012. <https://doi.org/10.1557/mrs.2012.275>
- Gu, Lei. "Low-frequency piezoelectric energy harvesting prototype suitable for the MEMS implementation." *Microelectronics Journal* 42, no. 2, pp. 277-282, 2011. <https://doi.org/10.1016/j.mejo.2010.10.007>
- Dhakar, L., Liu, H., Tay, F.E.H. and Lee, C., A new energy harvester design for high power output at low frequencies. *Sensors and Actuators A: Physical*, 199, pp.344-352. 2013. <https://doi.org/10.1016/j.sna.2013.06.009>
- Qiu, Jing, Yumei Wen, Ping Li, and Jin Yang. "Design and testing of piezoelectric energy harvester for powering wireless sensors of electric line monitoring system." *Journal of Applied physics* 111, no. 7, 2012. <https://doi.org/10.1063/1.3677771>
- Wang, Yingting, Liang Wang, Tinghai Cheng, Zhaoyang Song, and Feng Qin. "Sealed piezoelectric energy harvester driven by hyperbaric air load." *Applied Physics Letters* 108, no. 3, 2016. <https://doi.org/10.1063/1.4940199>
- Tang, G., Yang, B., Liu, J.Q., Xu, B., Zhu, H.Y. and Yang, C.S., Development of high performance piezoelectric d33 mode MEMS vibration energy harvester based on PMN-PT single crystal thick film. *Sensors and Actuators A: Physical*, 205, pp.150-155, 2014, <https://doi.org/10.1016/j.sna.2013.11.007>
- Jung, H.J., Jabbar, H., Song, Y. and Sung, T.H., Hybrid-type (d33 and d31) impact-based piezoelectric hydroelectric energy harvester for watt-level electrical devices. *Sensors and Actuators A: Physical*, 245, pp.40-48. 2016, <https://doi.org/10.1016/j.sna.2016.04.013>
- Seo, Y.H., Kim, B.H. and Choi, D.S., Piezoelectric micro power harvester using flow-induced vibration for infrastructure health monitoring applications. *Microsystem Technologies*, 21, pp. 169-172, 2015, <https://doi.org/10.1007/s11664-015-3959-2>
- Prasanta Kumar Panda, Benudhar Sahoo, M. Chandriah, Sreekumari Raghavan, Bindu Manoj, J. Ramakrishna and P. Kiran "Piezoelectric Energy Harvesting Using PZT Bimorphs and Multilayered Stacks" *Journal of ELECTRONIC MATERIALS*, Vol. 44, No. 11, 2015, <https://doi.org/10.1007/s11664-015-3959-2>
- Zeng, Z., Ren, B., Gai, L., Zhao, X., Luo, H. and Wang, D., 2016. Shear-mode-based cantilever driving low-frequency piezoelectric energy harvester using

- 0.67 Pb (Mg 1/3 Nb 2/3) O 3-0.33 PbTiO 3. IEEE transactions on ultrasonics, ferroelectrics, and frequency control, 63(8), pp.1192-1197, 2016, <https://DOI.10.1109/TUFFC.2016.2572308>
- Almuatasim Alomari and Ashok Batra "Experimental and Modelling Study of a Piezoelectric Energy Harvester Unimorph Cantilever Arrays" Sensors & Transducers, vol. 192, no. 9, pp. 37-43, 2015.
- Guan, M. and Liao, W.H., Design and analysis of a piezoelectric energy harvester for rotational motion system. Energy Conversion and Management, 111, pp. 239-244, 2016, <https://doi.org/10.1016/j.enconman.2015.12.061>
- Chew, Z. and Li, L., Design and characterisation of a piezoelectric scavenging device with multiple resonant frequencies. Sensors and Actuators A: Physical, vol. 162 no. 1, pp. 82-92. 2010, <https://doi.org/10.1016/j.sna.2010.06.017>
- Vasic, D., Chen, Y.Y. and Costa, F., Self-powered piezoelectric energy harvester for bicycle. Journal of Mechanical Science and Technology, 28, pp. 2501-2510. 2014, <https://doi.org/10.1007/s12206-014-0407-9>
- Kim, Taemin, Youngsu Ko, Chansei Yoo, Beomjin Choi, Seungho Han, and Namsu Kim. "Design optimisation of wide-band piezoelectric energy harvesters for self-powered devices." Energy Conversion and Management 225, 2020, <https://doi.org/10.1016/j.enconman.2020.113443>
- Shim, H.K., Sun, S., Kim, H.S., Lee, D.G., Lee, Y.J., Jang, J.S., Cho, K.H., Baik, J.M., Kang, C.Y., Leng, Y. and Hur, S., On a nonlinear broadband piezoelectric energy harvester with a coupled beam array. Applied Energy, 328, p.120129, 2022, <https://doi.org/10.1016/j.apenergy.2022.120129>
- Fan, Y., Ghayesh, M.H., Lu, T.F. and Amabili, M., Design, development, and theoretical and experimental tests of a nonlinear energy harvester via piezoelectric arrays and motion limiters. International Journal of Non-Linear Mechanics, 142, p.103974, 2022, <https://doi.org/10.1016/j.ijnonlinmec.2022.103974>
- Zhang, B., Zhou, H., Zhao, X., Gao, J. and Zhou, S., Design and experimental analysis of a piezoelectric energy harvester based on stacked piezoceramic for nonharmonic excitations. Energy, 282, p.128948, 2023, <https://doi.org/10.1016/j.energy.2023.128948>
- Pertin, O., Guha, K., Jakšić, O., Jakšić, Z. and Iannacci, J., Investigation of nonlinear piezoelectric energy harvester for low-frequency and wideband applications. Micromachines, 13(9), p.1399, 2022, <https://doi.org/10.3390/mi13091399>
- Machado, S.P., Febbo, M. and Osinaga, S.M., Double impact-based piezoelectric energy harvester for low-frequency operation. IEEE Sensors Journal, 23(2), pp.1081-1090, 2022, <https://DOI.10.1109/JSEN.2022.3226537>
- Pan, J., Zhang, X., Qin, W., Xu, H., Tian, H., Zhu, F. and Guo, Y., A broadband zigzag-shaped energy harvester for both wind energy and vibration energy: modeling and experimental verification. Journal of Physics D: Applied Physics, 56(14), p.144002, 2023, <https://DOI.10.1088/1361-6463/acbc30>
- Yu, H., Zhang, X., Shan, X., Hu, L., Zhang, X., Hou, C. and Xie, T., A novel bird-shape broadband piezoelectric energy harvester for low frequency vibrations. Micromachines, 14(2), p.421, 2023, <https://doi.org/10.3390/mi14020421>